Current GISS Global Surface Temperature Analysis

J. Hansen, R. Ruedy, M. Sato, and K. Lo
NASA Goddard Institute for Space Studies, New York, New York, USA

Abstract. We update the Goddard Institute for Space Studies (GISS) analysis of global surface temperature change. We use satellite nightlight measurements to identify measurement stations located in extreme darkness. These stations are used to adjust temperature trends of urban and peri-urban stations for non-climatic factors and to help verify that urban effects on analyzed global change are small. As the GISS analysis combines available sea surface temperature records with meteorological station measurements, we test alternative choices for the ocean record, showing that global temperature change is sensitive to estimated temperature change in polar regions where observations are limited. We compare global temperature reconstructions of GISS, NCDC, and HadCRUT. We conclude that global temperature continued to rise rapidly in the past decade, despite large year-to-year fluctuations associated with the El Nino-La Nina cycle of tropical ocean temperature.

1. Introduction

Analyses of global surface temperature change are routinely carried out by several groups, including the NASA Goddard Institute for Space Studies, the NOAA National Climatic Data Center (NCDC), and a joint effort of the Hadley Research Centre and the University of East Anglia Climate Research Unit (HadCRUT). These analyses are not independent, as they must use much the same input observations. However, the multiple analyses provide useful checks because they employ different ways of handling data problems such as incomplete spatial and temporal coverage and non-climatic influences on measurement station environment.

Here we describe the current GISS analysis of global surface temperature change. We first provide background on why and how the GISS method was developed and then describe the input data that go into our analysis. We discuss sources of uncertainty in the temperature records and provide some insight about the magnitude of the problems via alternative choices input data and adjustments to the data. We discuss a few of the salient features in the resulting temperature reconstruction and compare our global mean temperature change with that obtained in the NCDC and HadCRUT analyses. Given our conclusion that global warming is continuing unabated, and that this conclusion differs from some popular conceptions, we discuss reasons for such perceptions including the influence of short-term weather and climate fluctuations.

2. Background of GISS Analysis Method

GISS analyses of global surface temperature change were initiated by one of us (JH) in the late 1970s and first published in 1981 [*Hansen et al.*, 1981]. The objective was an estimate of global temperature change that could be compared with expected global climate change in response to known or suspected climate forcing mechanisms such as atmospheric carbon dioxide, volcanic aerosols, and solar irradiance changes.

A principal question at that time was whether there were sufficient stations in the Southern Hemisphere to allow a meaningful evaluation of global temperature change. The supposition in the GISS analysis was that an estimate of global temperature change with useful accuracy should be possible because seasonal and annual temperature anomalies, relative to a long-term average (climatology), present a much smoother geographical field than temperature

itself. For example, when New York City has an unusually cold winter, it is likely that Philadelphia is also colder than normal.

The correlation of temperature anomaly time series for neighboring stations was illustrated by *Hansen and Lebedeff* [1987] as a function of station separation for different latitude bands. The average correlation coefficient was shown to remain above 50 percent to distances of about 1200 km at most latitudes, but in the tropics the correlation falls to about 35 percent at station separation of 1200 km. The GISS analysis specifies the temperature anomaly at a given location as the weighted average of the anomalies for all stations located within 1200 km of that point, with the weight decreasing linearly from unity for a station located at that point to zero for stations located 1200 km or further from the point in question.

The GISS analysis thus interpolates among station measurements and extrapolates anomalies as far as 1200 km into regions without measurement stations. Resulting regions with defined temperature anomalies are used to calculate a temperature anomaly history for large latitude zones. The global temperature anomaly time series is then calculated as the average for all zones, with each zone weighted by its true (complete) area.

Hansen and Lebedeff [1987] calculated an error estimate due to incomplete spatial coverage of stations using a global climate model that was shown to have realistic spatial and temporal variations of temperature anomalies. The average error was found by comparing global temperature variations from the spatially and temporally complete model fields with the results when the model was sampled only at locations and times with measurements. Calculated errors increased toward earlier times as the area covered by stations diminished, with the errors becoming comparable in magnitude to estimated global temperature changes at about 1880. Thus we restrict GISS temperature anomaly estimates to post-1880.

The GISS analysis uses 1951-1980 as the base period. The United States National Weather Service uses a three-decade period to define "normal" or average temperature. At the time we began our global temperature analyses and comparisons with climate models that climatology period was 1951-1980. It seems best to keep the base period fixed, because many graphs have been published with that choice for climatology. It is a good choice for another reason: many of today's adults grew up during that period, so they can remember what climate was like then. Besides, a different base period only alters the zero point for anomalies, without changing the magnitude of the temperature change over any given period.

GISS analyses beginning with *Hansen et al.* [1999] include a homogeneity adjustment to minimize local (non-climatic) anthropogenic effects on measured temperature change. Such effects are usually largest in urban locations where buildings and energy use often cause a warming bias. Local anthropogenic cooling can also occur, for example from irrigation and planting of vegetation, but on average these effects are probably outweighed by urban warming. The homogeneity adjustment procedure [Figure 3 of *Hansen et al.*, 1999] changes the long-term temperature trend of an urban station to make it agree with the mean trend of nearby rural stations. The effect of this adjustment on global temperature change was found to be small, less than 0.1°C for the past century. Discrimination between urban and rural areas was based on the population of the city associated with the meteorological station. Location of stations relative to population centers varies, however, so in the present paper we use the intensity of high resolution satellite nightlight measurements to specify which stations are in population centers and which stations should be relatively free of urban influence.

The GISS temperature analysis has been available for many years on the GISS web site (www.nasa.giss.gov), including maps, graphs and tables of the results. The analysis is updated monthly using several data sets compiled by other groups from measurements at meteorological

stations and satellite measurements of ocean surface temperature. Ocean data in the pre-satellite era is based on measurements by ships and buoys. The computer program that integrates these data sets into a global analysis is freely available on the GISS web site.

Here we describe the current GISS analysis and present several updated graphs and maps of global surface temperature change. We compare our results with those of HadCRUT and NCDC, the main purpose being to investigate differences in recent global temperature trends and the ranking of annual temperatures among different years.

3. Input Data

The current GISS analysis employs three independent input data streams that are publicly available on the internet and updated monthly. In addition the analysis requires a data set for ocean surface temperature measurements in the pre-satellite era; we now show results using alternative choices for pre-satellite ocean data Measurements for land areas are of surface air temperature, which is usually measured at a height of two meters. Ocean measurements are of the water temperature at or near the sea surface. Although air and water temperatures differ, temperature change of slightly different surface levels should be similar in most situations because of tight coupling between the surface and near surface air. We refer to this combined data product as surface temperature change.

3.1. Meteorological Station Measurements

The source of monthly mean station measurements for our current analysis is the Global Historical Climatology Network (GHCN) version 2 of *Peterson and Vose* [1997], which is available monthly from NCDC. GHCN includes data from about 7000 stations. We use only those stations that have a period of overlap with neighboring stations (within 1200 km) of at least 20 years (see Figure 2 of *Hansen et al*., 1999), which reduces the number of stations used in our analysis to about 6300.

We use the unadjusted version of GHCN. However, note that a subset of GHCN, the United States Historical Climatology Network (USHCN), has been adjusted via a homogenization intended to remove urban warming and other artifacts [*Karl et al*., 1990; *Peterson and Vose,* 1997]. Also bad data in GHCN were minimized at NCDC [*Peterson and Vose,* 1997; *Peterson et al.*, 1998b] via checks of all monthly mean outliers that differed from their climatology by more than 2.5 standard deviations. About 15 percent of these outliers were eliminated for being incompatible with neighboring stations, with the remaining 85 percent being retained.

The current GISS analysis adjusts the long-term temperature trends of urban stations based on neighboring rural stations, and we correct discontinuities in the records of two specific stations as described below. Our standard urban adjustment now utilizes satellite observations of nightlights to identify whether stations are located in rural or urban areas. The urban adjustment, described below, is carried out via our published computer program and the publicly available nightlight data set.

Our analysis also continues to include specific adjustments for two stations, as described by *Hansen et al.* [1999], these stations being located in isolated regions where sufficient neighboring stations are not available for the automatic adjustment. The two stations have obvious discontinuities that would give rise to artificial global warming without a homogeneity adjustment. The stations, St. Helena in the tropical Atlantic Ocean and Lihue, Kauai, in Hawaii, are located on islands with few if any neighboring stations, so their records have a noticeable

impact on analyzed regional temperature change. The St. Helena station, based on metadata in MCDW records, was moved from 604 m to 436 m elevation between August 1976 and September 1976. Thus, assuming a temperature lapse rate of 6°C/km, we added 1°C to St. Helena temperatures before September 1976. Lihue had an obvious discontinuity in its temperature record around 1950. On the basis of minimizing the discrepancy with its few neighboring stations, we added 0.8°C to Lihue temperatures prior to 1950.

In the current monthly updates of the GISS analysis when we find what seems to be a likely error in a station record, our procedure is to report the problem to NCDC for their consideration and possible correction of the GHCN record. Our rationale is that verification of correct data entry from the original meteorological source is a person-intensive activity that is best handled by NCDC with its existing communications network. Also it seems better not to have multiple versions of the GHCN data set in the scientific community.

The contiguous United States presents special homogeneity problems. One problem is the bias introduced by change in the time of daily temperature recording [*Karl et al.*, 1986], a problem that does not exist in the temperature records from most other nations. High energy use, built up local environments, and land use changes also cause homogeneity problems [*Karl et al.*, 1990]. The adjustments included by NCDC in the current USHCN data set [version 2, *Menne et al.*, 2009] should reduce these problems. As a test of how well urban influences have been minimized, we illustrate below the effect of our nightlight-based urban adjustment on the current USHCN data set.

3.2. Antarctic Research Station Measurements

Measurements at Antarctic research stations help fill in what would otherwise be a large hole in the GHCN land-based temperature record. Substantial continuous data coverage in Antarctica did not begin until the International Geophysical Year (1957). However, the period since 1957 includes the time of rapid global temperature change that began in about 1980.

The GISS analysis uses the Scientific Committee on Antarctic Research (SCAR) monthly data [*Turner et al.*, 2004], which are publicly available.

3.3. Ocean Surface Temperature Measurements

Our standard global land-ocean temperature index uses a concatenation of the Hadley Research Centre ship-based analysis of sea surface temperatures (HadISST1) [*Rayner et al.*, 2003] for 1880-1981 and satellite measurements of sea surface temperature for 1982-present (OISST.v2) [*Reynolds et al.*, 2002]. The satellite measurements are calibrated with the help of ship and buoy data [*Reynolds et al.*, 2002].

Ocean surface temperatures have their own homogeneity issues. Measurement methods changed over time as ships changed, most notably with a change from measurements of bucket water to engine intake water. Homogeneity adjustments have been made to the ship-based record [*Parker et al.*, 1995; *Rayner et al.*, 2003], but these are necessarily imperfect. The spatial coverage of ship data is poor in the early 20th century and before. Also it has been shown that changes in ship measurements during and after World War II cause an instrumental artifact that contributes to the relative peak of ocean temperature in the HadISST1 data set in the early 1940s [*Thompson et al.*, 2008]. Ocean coverage and the quality of sea surface temperature measurements have been better since 1950 and especially during the era of satellite ocean data, i.e., since 1982. Satellite data, however, also have their own sources of uncertainty, despite their high spatial resolution and broad geographical coverage.

Thus we compare the global temperature change obtained in our standard analysis, which concatenates HadISST1 and OISST.v2, with results from our analysis program using alternative ocean data sets. Specifically, we compare our standard case with results when the ocean data is replaced by the Extended Reconstructed SST (ERSST.v3) [*Smith et al.*, 2008] for the full period 1880-present, and also when HadISST1 is used as the only ocean data for the full period 1880-present. In the Supplementary Material we compare the alternative ocean data sets themselves over regions of common data coverage to help isolate differences among input SSTs as opposed to differences in the area covered by ocean data.

4. Urban Adjustments

Station location in the meteorological data records is provided with a resolution of 0.01 degrees of latitude and longitude, corresponding to a distance of about 1 km. This resolution is useful for investigating urban effects on regional atmospheric temperature. Much higher resolution would be needed to check for local problems with the placement of thermometers relative to possible building obstructions, for example. In many cases such local problems are handled via site inspections and reported in the "metadata" that accompanies station records, as discussed by *Karl and Williams* [1987], *Karl et al.* [1989], and *Peterson et al.* [1998a].

Of course the thousands of meteorological station records include many with uncorrected problems. The effect of these problems tends to be reduced by the fact that they include errors of both signs. Also problems are usually greater in urban environments, so an urban adjustment based on nightlights should tend to reduce the effect of otherwise unnoticed non-climatic effects.

We use a nightlight radiance data set [*Imhoff et al.*, 1997] that is publicly available [http://www.ngdc.noaa.gov/dmsp/download_rad_cal_96-97.html] (measurements made between March 1996 and February 1997)] at a resolution of 30" x 30", which is a linear scale of about 1 km. In Figure 1(a) the global radiances are shown after averaging to 30' x 30' resolution, i.e., a pixel (resolution element) in Figure 1(a) is an average over 3600 high resolution pixels. This averaging reduces the maximum radiance from about 3000 $\mu W/m^2/sr/\mu m$ to about 670 $\mu W/m^2/sr/\mu m$.

Imhoff et al. [1997] investigated the relation between nightlight radiances and population density in the United States. We find that radiances of less than 32 $\mu W/m^2/sr/\mu m$ correspond well with the "unlit" category of *Imhoff et al*. [1997] within the United States, as can be seen by comparing Figure 1(b) here with Plate 1 of *Hansen et al.* [2001]. The "unlit" regions, according to *Imhoff et al* [1997] correspond to populations densities of about 0.1 persons/ha or less in the United States.

The relation between population and nightlight radiance in the United States is not valid in the rest of the world, as energy use per capita is higher in the United States than in most countries. However, energy use is probably a better metric than population for estimating urban influence, so we employ nightlight radiance of 32 $\mu W/m^2/sr/\mu m$ as the dividing point between rural and urban areas in our global nightlight test of urban effects. Below we show, using data for a region with very dense station coverage, that use of a much more stringent for darkness does not significantly alter the results.

We first compare two alternatives for the urban correction. One case uses the definition of rural stations used by *Hansen et al.* [1999], i.e., stations associated with towns of population less than 10,000 (population data available at ftp://ftp.ncdc.noaa.gov/pub/data/ghcn/v2). The second case defines rural stations as those located in a region with nightlight radiance less than 32 $\mu W/m^2/sr/\mu m$.

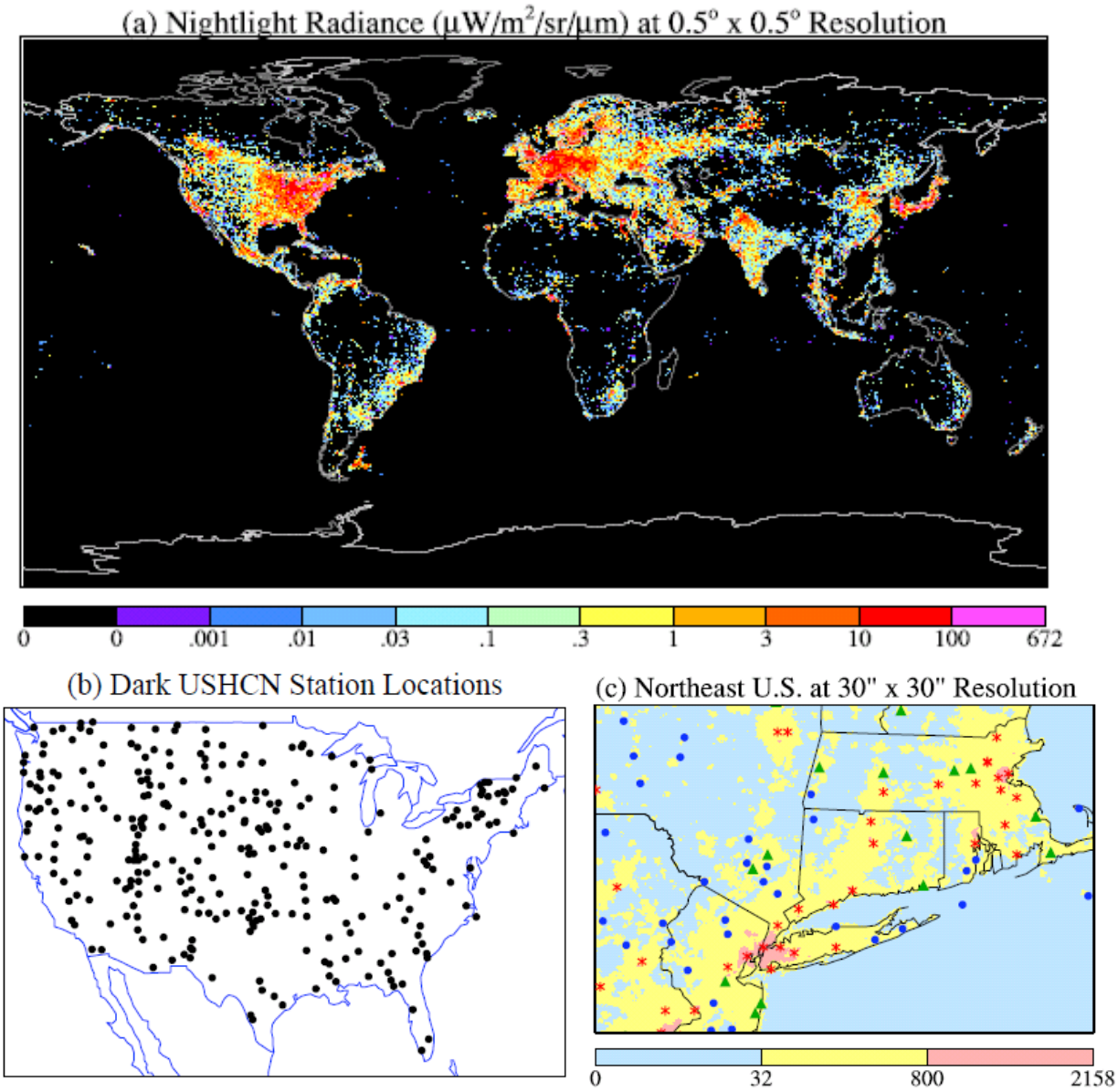

Figure 1. (a) Satellite-observed nightlight radiances at a spatial resolution of 30 minutes x 30 minutes, (b) locations of USHCN stations in extreme darkness, nightlight radiance less than 1 μW/m^2/sr/μm, and (c) a region shown at the data resolution of 30 seconds x 30 seconds [*Imhoff et al*., 1997]. Blue dots indicate meteorological stations associated with towns having population less than 10,000. In our new standard nightlight treatment stations in the yellow and pink regions are adjusted for urban effects.

This nightlight criterion is stricter than the population criterion in the United States, i.e., many sites classified as rural based on population below 10,000 are classified as urban based on nightlight brightness, as illustrated by the fact that some of the blue dots (towns of population less than 10,000) in Figure 1c fall within the urban areas defined by nightlights (yellow area). However, as we will see, the opposite is true in places such as Africa, i.e., a population criterion of less than 10,000 results in fewer rural stations than the nightlight criterion.

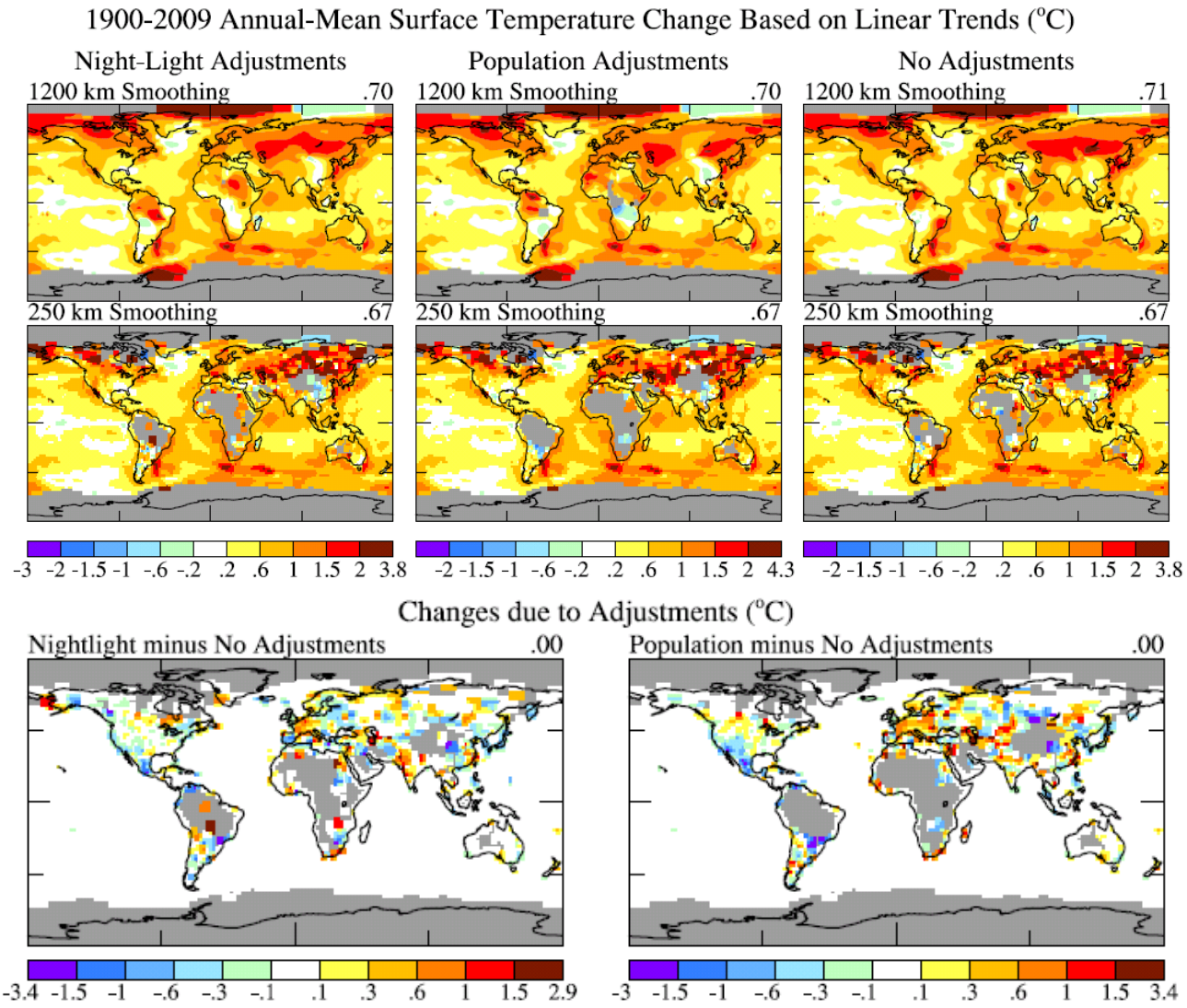

Figure 2. Comparison of alternative urban adjustments. The top row uses the standard 1200 km radius of influence for each station while the second row reduces the radius of influence to 250 km, so that the influence of adjustments on individual stations can be ascertained. The temperature change due to the adjustments is shown in the two bottom maps.

Our adjustment of urban station records uses nearby rural stations to define the long-term trends while allowing the local urban station to define high frequency variations, nominally as described by *Hansen et al.* [1999], but with details as follows. If an urban station has at least three rural stations within 500 km, all of these are used for the adjustment with closer stations receiving greater weight, as described above. If there are not three stations within 500 km, but there are three or more stations within 1000 km, these stations are used for the adjustment. The mean temperature trend of the rural stations is computed as a two-segment broken line, as in *Hansen et al.* [1999] but the knee of the broken line is variable (rather than being fixed at 1950) chosen so as to minimize the difference between the urban and rural records.

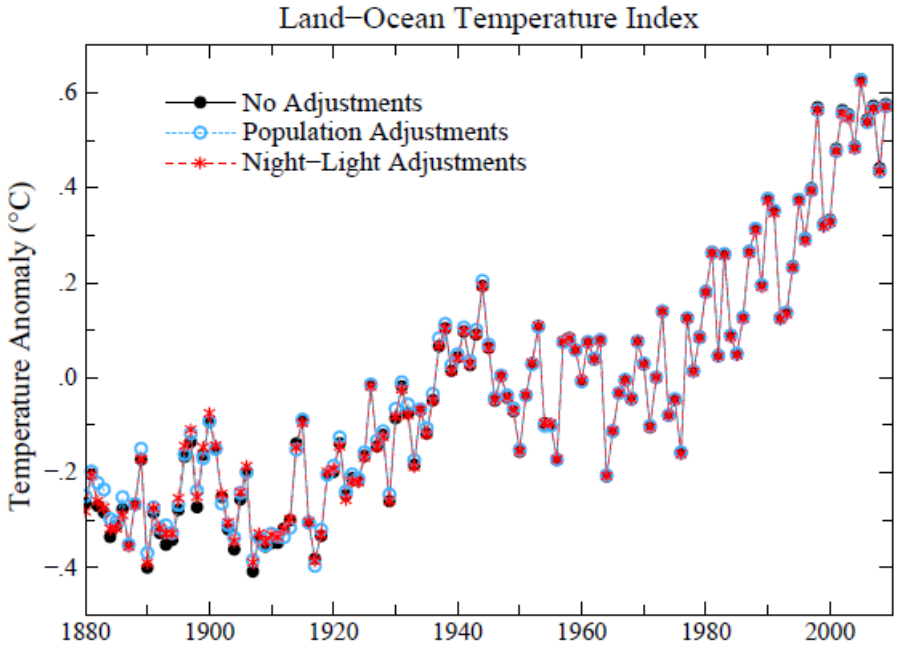

Figure 3. Global-mean annual-mean land-ocean temperature index for three alternative treatments of the urban adjustment.

Figure 2 shows the resulting temperature change over the period 1900-2009 for urban adjustment based on nightlights, urban adjustment based on population, and no urban adjustment. The effect of urban adjustment on global temperature change is only of the order of 0.01°C for either nightlight or population adjustment. The small magnitude of the urban effect is consistent with results found by others [*Karl et al.*, 1988; *Jones et al.*, 1990; *Peterson et al.*, 1999; *Peterson*, 2003; *Parker*, 2004]. Our additional check is useful, however, because of the simple reproducible way that nightlights define rural areas. We previously used this nightlight method [*Hansen et al.*, 2001], but only for the contiguous United States.

The most noticeable effect of the urban adjustment in Figure 2 is in Africa and includes changes of both signs. The large local changes are not due to addition of an urban correction to specific stations, but rather to the deletion of urban stations because of the absence of three rural neighbors. African station records are especially sparse and unreliable [*Peterson et al.*, 1998b; *Christy et al.*, 2009]. Thus the large local temperature changes between one adjustment and another may have more to do with variations in station reliability rather than urban warming. Given the paucity of reliable station records in Africa and South America [*Peterson et al.*, 1997], it is difficult to have confidence in the illustrated temperature trends on those continents.

Figure 3 compares the global mean temperature versus time for the two alternative urban adjustments and no urban adjustment. The main conclusion to be drawn is that the differences among the three curves are small. Nevertheless, we know that the adjustment is substantial for some urban stations, so it is appropriate to include an urban adjustment.

How can we judge whether the nightlight or population adjustment is better in the sense of yielding the most realistic result? One criterion might be based on which one yields more realistic continuous meteorological patterns for temperature anomaly patterns. Nightlights arguably do very slightly better based on that criterion (Figure 2). Independently, we expect nightlight intensity to be a better indication than population of urban heat generation. Nightlights also preserve a greater area with defined temperature anomalies (Figure 2). Finally,

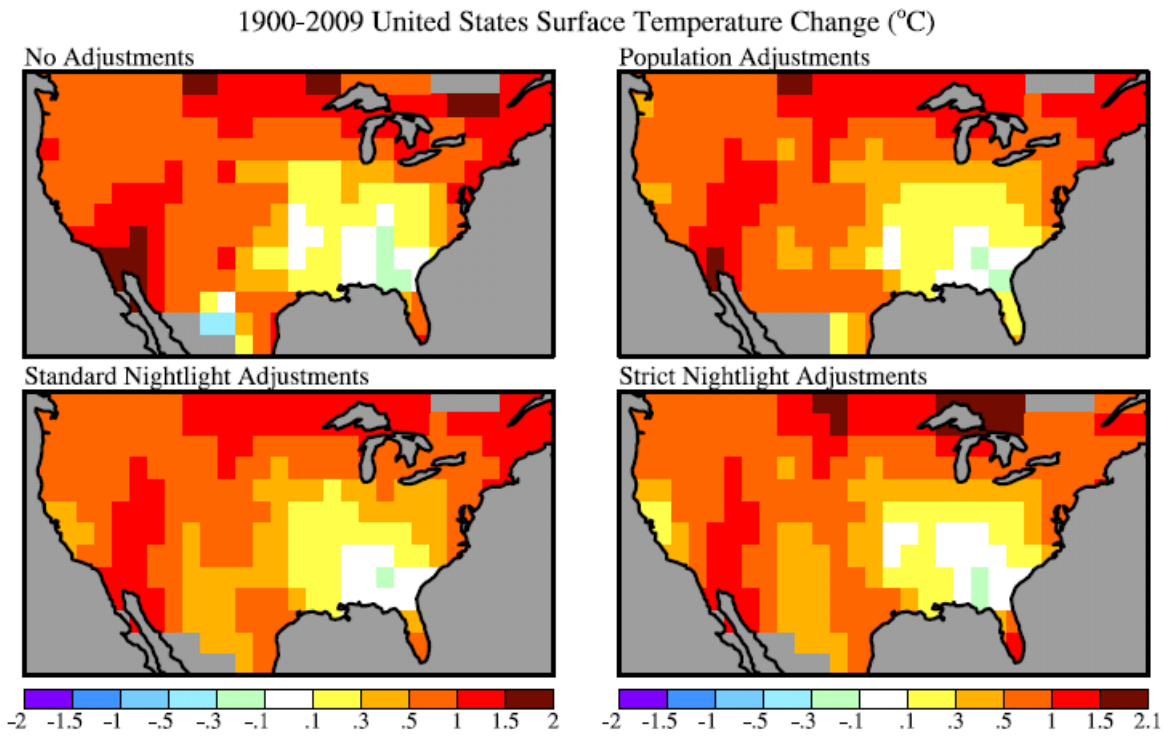

Figure 4. Temperature change in the United States for alternative choices of urban adjustment.

stations can be more accurately associated with nightlight intensity (within about 1km) than with population, and the nightlight data are easily accessible, so anyone can check our analysis.

For these reasons, beginning in January 2010 the standard GISS analysis employs global nightlights in choosing stations to be adjusted for urban effects. Use of nightlights is a well-defined objective approach for urban adjustment, and the nightlight data set used for the adjustment is readily available (see http address above). In the future, as additional urban areas develop, it will be useful to employ newer satellite measurements.

The small urban correction is somewhat surprising, even though it is consistent with prior studies. We know, for example, that urban effects of several degrees exist in some cities such as Tokyo, Japan and Phoenix, Arizona, as illustrated in Figure 3 of *Hansen et al.* [1999]. Although such stations are adjusted in the GISS analysis, is it possible that our 'rural' stations themselves contain substantial human-made warming? There is at least one region, the United States, where we can do a stricter test of urban warming, because of the high density of meteorological stations. The United States is a good place to search for greater urban effects, because of its high energy use and a consequent expectation of large urban effects.

In Figures 4 and 5 we compare no adjustment, population adjustment, and two nightlight adjustments. The standard nightlight adjustment defines rural as nightlight radiance less than 32 $\mu W/m^2/sr/\mu m$ and stringent darkness is the lowest radiance class in the satellite data set, beneath the detection limit of about 1 $\mu W/m^2/sr/\mu m$. There were about 300 stations in the contiguous United States meeting this strict darkness criterion (Figure 1b), sufficient to yield a filled-in United States temperature anomaly map even with the station radius of influence set at 250 km. We use the 250 km radius of influence to provide higher resolution in Figure 4, compared with 1200 km radius of influence, and we exclude smoothing from the plotting package so that results are shown at the 2°×2° resolution of the calculation, thus allowing more quantitative inspection.

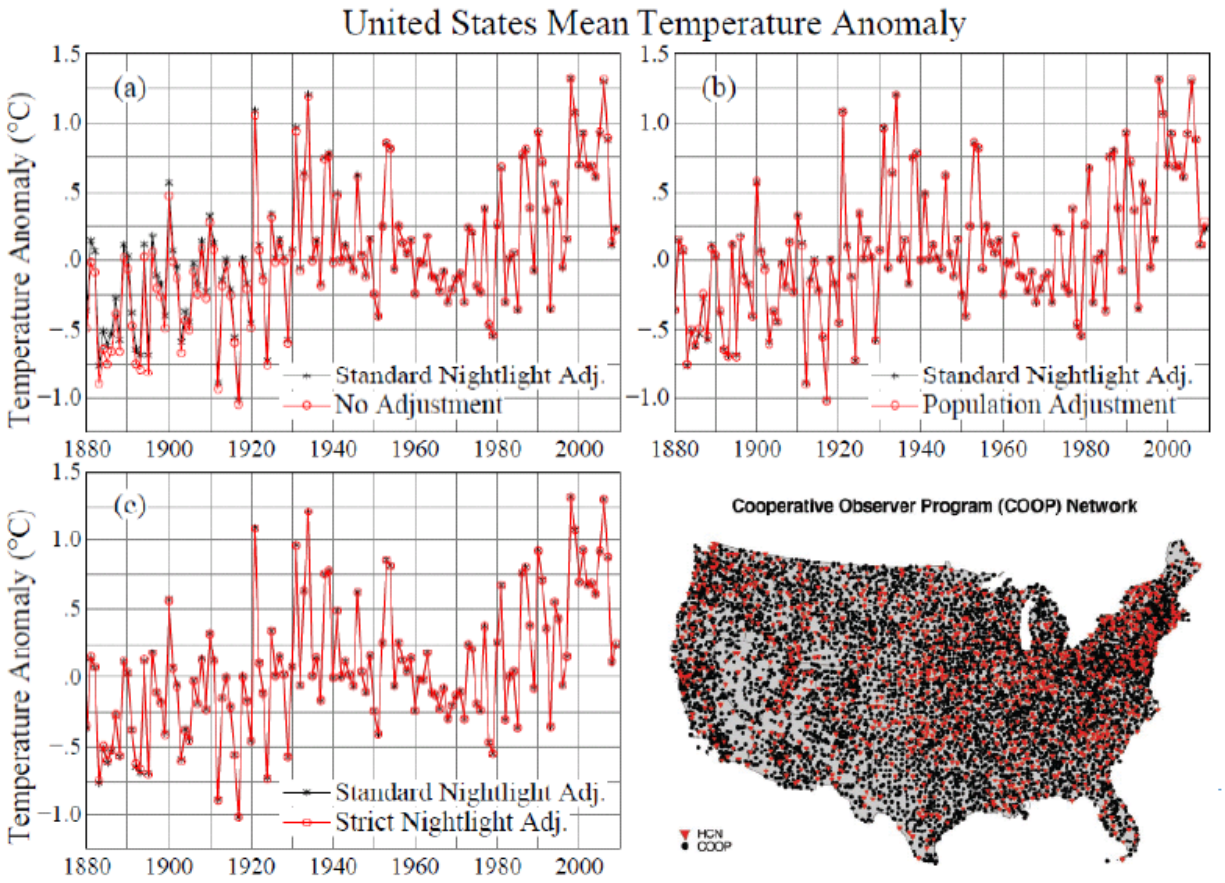

Figure 5. Comparisons of mean temperature anomalies in the contiguous 48 United States for the standard GISS nightlight adjustment and alternative. The map on the lower right shows the high density of meteorological stations in the United States, with red being stations in the U.S. Historical Climatology Network and black being Cooperative stations [*Menne et al.*, 2009].

The largest urban adjustment is in the Southwest United States, where a warming bias is removed. In a few locations the adjustment yields greater warming, which can result from either the spatial smoothing inherent in adjusting local trends to match several neighboring stations or neighboring rural stations that have greater warming than the urban station . The standard nightlight adjustment removes slightly more warming than does the population adjustment. The important conclusion is that the strict nightlight adjustment has no significant additional effect, compared with the standard nightlight adjustment. The 1900-2009 temperature change over the contiguous United States, based on linear fit to the data in Figure 5, is 0.70°C (no adjustment), 0.64°C (population adjustment), 0.63°C (standard nightlight adjustment), and 0.64°C (strict nightlight adjustment). If only USHCN stations are employed (as in NCDC analyses) we find a 1900-2009 temperature change of 0.73°C (no adjustment) and 0.65°C (standard nightlight adjustment).

Global temperature change in this paper, unless indicated otherwise, is based on the standard nightlight adjustment. We conclude, based on results reported here and the other papers we referenced, that unaccounted for urban effects on global temperature change are small in comparison to the ~0.8°C global warming of the past century. Extensive confirmatory evidence (such as glacier retreat and borehole temperature profiles) is provided by *IPCC* [2007].

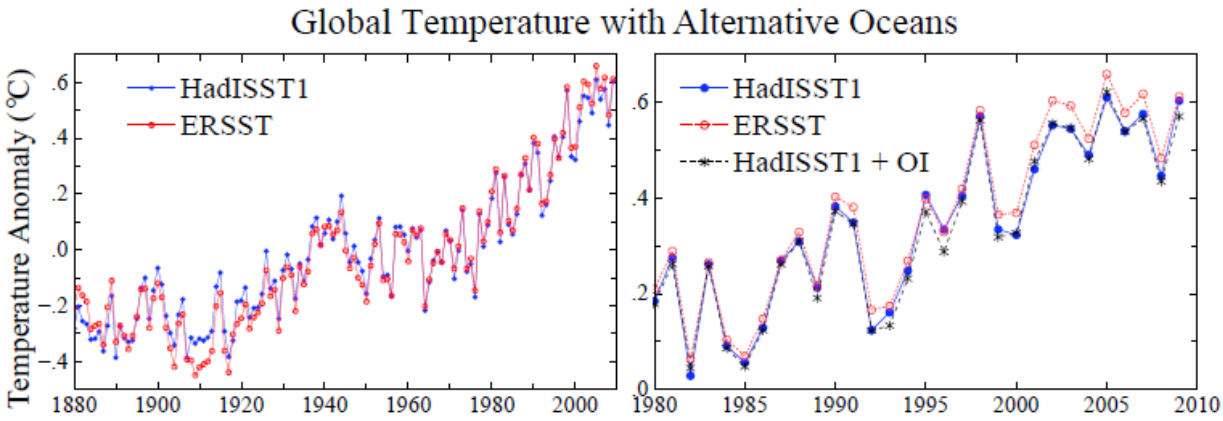

Figure 6. Global temperature change in the GISS global analysis for alternative choices of sea surface temperature.

5. Alternative Ocean Data Sets

Figure 6 compares global temperature change for three choices of ocean surface temperature: (1) HadISST1 [*Rayner et al.*, 2003] for 1880-1981 and OISST.v2 [*Reynolds et al.*, 2002] for 1982-present, (2) ERSST.v3 [*Smith et al.*, 2008] for the full period 1880-present, (3) HadISST1 for 1880-2008. In all three cases the land data is based on the GISS analysis of GHCN and Antarctic (SCAR) data.

The first of the ocean data sets, the combination HadISST1+OISST.v2, is used in the GISS analysis for our standard land-ocean temperature index. Results based on HadISST1 alone and HadISST1+OISST.v2 are in close agreement in the 1982-present period during which they might differ (Figure 6b). We use OISST for the satellite era, as opposed to HadISST1, in part because OISST is available weekly in near real time.

ERSST, a newer SST analysis covering the period 1880 to the present, is also available in near real time. SST values in data sparse regions in ERSST are filled in by NCDC using statistical methods, dividing the SST anomaly patterns into low-frequency (decadal scale) anomalies, by averaging and filtering available data points, and high-frequency residual anomalies [*Smith et al.*, 2008]. The concept is that the SST reconstruction may be improved by constraining temperature anomaly fields toward realistic modes of variability.

ERSST yields 0.04°C greater global warming (based on linear trends) than HadISST1 or HadISST1+OISST over the period 1880-2009 (Figure 6a). Over 1980-2009 ERSST yields global warming about 0.03°C greater than either HadISST1 or HadISST1+OISST (Figure 6b). Figure 7 illustrates the geographical distribution of the differences between ERSST and the other data sets. Satellite data used for OISST has high spatial and temporal resolution, but that does not necessarily lead to more accurate temperature trends. Aerosols and clouds, for example, cause calibration difficulties for the satellite measurements [*Reynolds et al.*, 2002].

It is apparent that the greater warming in ERSST on the century time scale occurs primarily in the South Pacific and South Atlantic oceans. The difference between the two reconstructions is large enough in the Pacific Ocean that it may be possible to discriminate between them based on proxy measures of climate change, for example from ocean sediments.

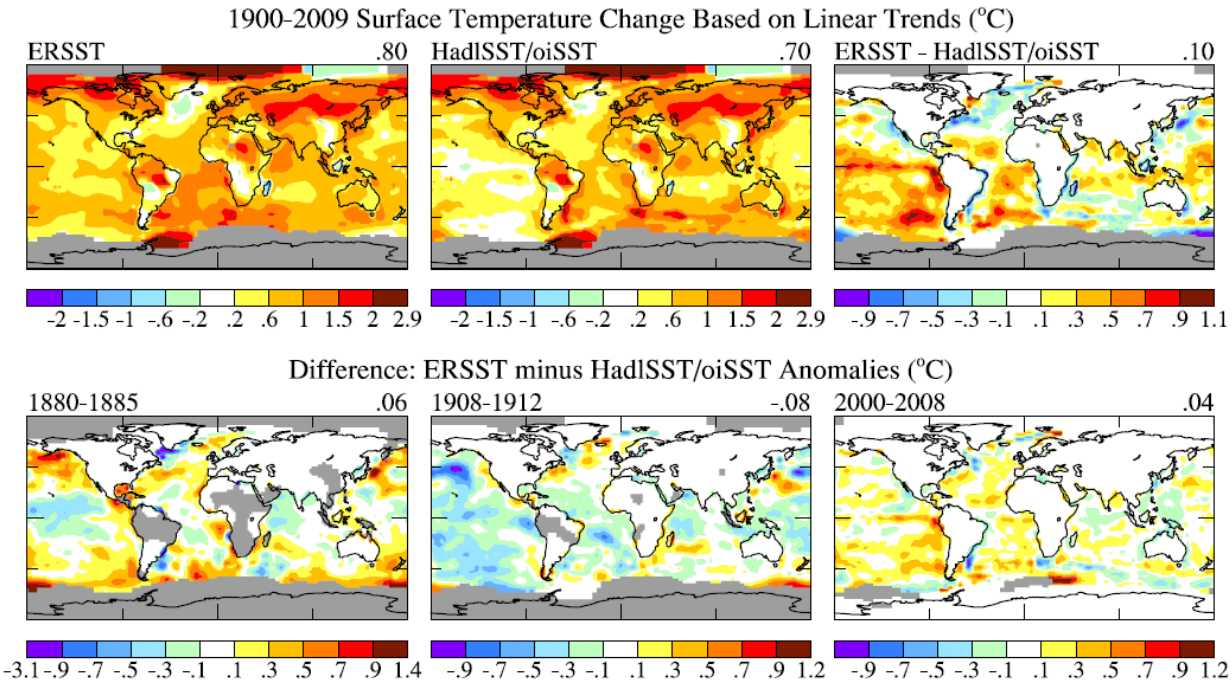

Figure 7. Temperature change in the GISS global analysis using ERSST and HadISST1+OISST and differences in specific periods.

A newer Hadley SST data set, HadSST2 (*Rayner et al.*, 2006) has cooler SSTs in 1908-1912, comparable to the lower temperatures in ERSST. Both HadSST2 and ERSST use newer versions of the International Comprehensive Ocean-Atmosphere Data Set [ICOADS; *Worley et al.*, 2005]. Presumably the newer ICOADS data is superior, as it is based on more data with better geographical coverage. However, the HadSST2 resolution (5°×5°) is too crude for our purposes. HadISST1 has 1°×1° resolution and ERSST has 2°×2° resolution.

In data-rich areas such as the North Atlantic Ocean in recent years there are sufficient in situ measurements to help assess the accuracy of the alternative SST reconstructions. *Hughes et al.* [2009] found better agreement of HadISST1+OISST than ERSST with spatial variability of in situ observations in recent decades that include high spatial and temporal resolution. Thus this assessment is dependent mainly on small scale variability and does not necessarily mean that ERSST has not improved the large-scale long-term temperature trends.

In recent years, as shown for 2000-2008 in the lower right part of Figure 7, the greater warming in ERSST occurs especially in the Eastern Pacific Ocean. These differences between the alternative ocean analyses are large enough that it may be possible to use *in situ* measurements to help determine which ocean temperature reconstruction is more accurate.

Until better assessments of the alternative SST data sets exist, the GISS global analysis will be made available for both HadISST1 and ERSST, in both cases with these long-term data sets concatenated with OISST for 1982-present. HadISST1+OISST will continue to be our standard product unless and until verifications show ERSST to be superior.

We compare the alternative ocean data sets over their regions of common data coverage in our Supplementary Material. Differences among the data sets, although noticeable, are less than uncertainties described by the data providers. The differences are also small enough that the choice of ocean data set does not alter conclusions of our paper.

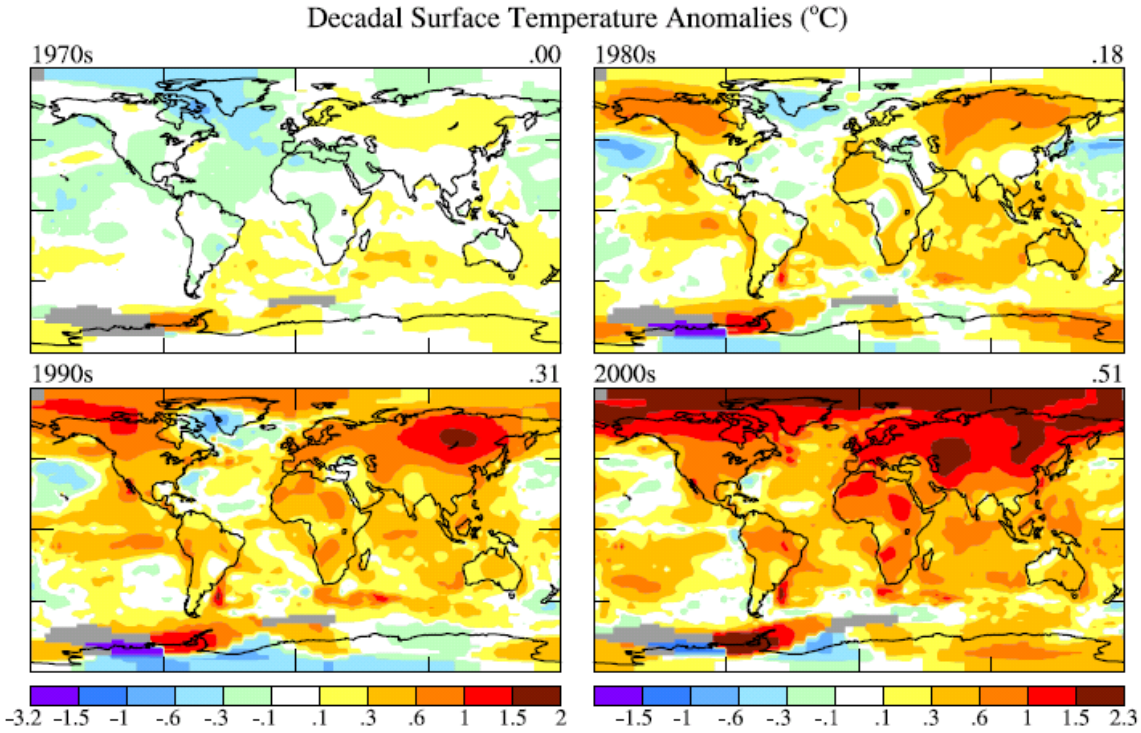

Figure 8. Decadal surface temperature anomalies relative to 1951-1980 base period.

6. Current GISS Surface Temperature Analysis

The results in this section use HadISST1+OISST with the switch to OI in 1982. A smooth concatenation is achieved by making the 1982-1992 OISST mean anomaly at each gridbox identical to the HadISST1 1982-1992 mean for that gridbox. When ERSST is substituted for HadISST1 the results are very similar, but with slightly larger global warming. Both results are available on our website.

Figure 8 shows the global surface temperature anomalies for the past four decades, relative to the 1951-1980 base period. On average, successive decades warmed by 0.17°C. The warming of the 1990s (0.13°C relative to the 1980s) was reduced by the temporary effect of the 1991 Mount Pinatubo volcanic eruption.

Warming in these recent decades is larger over land than over ocean, as expected for a forced climate change, because the ocean responds more slowly than the land due to the ocean's large thermal inertia. Warming during the past decade is enhanced, relative to the global mean, by about 50 percent in the United States, a factor of 2-3 in Eurasia, and a factor of 3-4 in the Arctic and the Antarctic Peninsula.

Warming of the ocean surface has been largest over the Arctic Ocean, second largest over the Indian and Western Pacific Oceans, and third largest over most of the Atlantic Ocean. Temperature changes have been small and variable in sign over the North Pacific Ocean, the Southern Ocean, and the regions of upwelling off the west coast of South America.

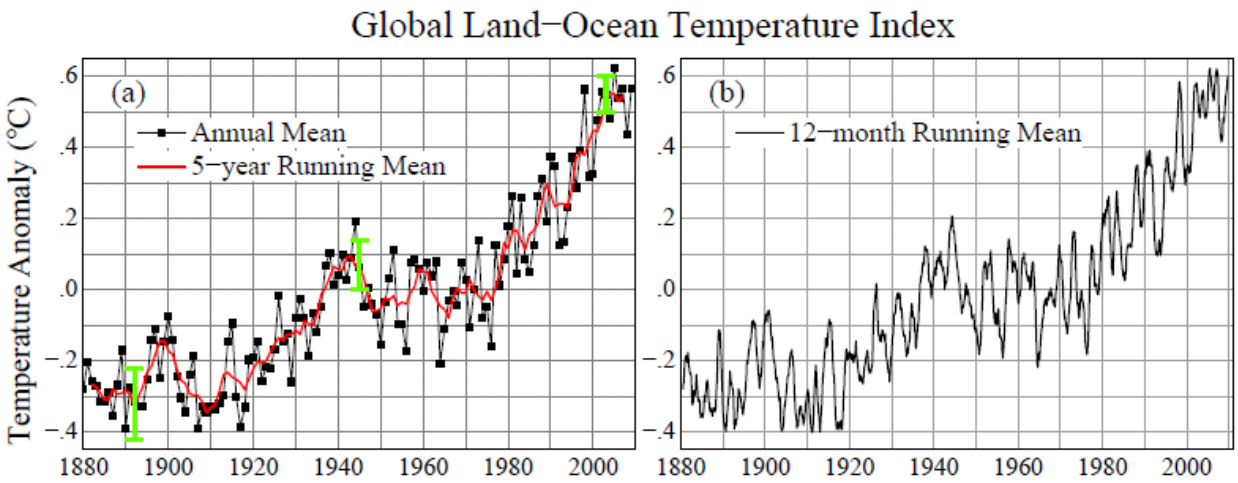

Figure 9. Global surface temperature anomalies relative to 1951-1980 mean for (a) annual and 5-year running means through 2009, and (b) 12-month running mean through February 2010.

Figure 9a updates the GISS global annual and 5-year mean temperatures through 2009. Results differ slightly from our prior papers because of our present use of the global nightlights to adjust for urban effects, but the changes are practically imperceptible. The nightlight adjustment reduces the 1880-2009 global temperature change by an insignificant 0.004°C relative to the prior population-based urban adjustment.

Global temperature in the past decade was about 0.8°C warmer than at the beginning of the 20th century (1880-1920 mean). Two-thirds of the warming has occurred since 1975.

Figure 9a has become popular, eagerly awaited by some members of the public and the media. An analogous graph, often in the form of a histogram is made available each year by the Hadley Centre/University of East Anglia Climate Research Unit and by the NOAA National Climatic Data Center.

We suggest, however, that a more informative and convenient graph is the 12-month running mean global temperature (Figure 9b). From a climate standpoint there is nothing special about the time of year at which the calendar begins. The 12-month running mean entirely removes the seasonal cycle just as well at any time of year.

The 12-month running mean temperature anomaly (Figure 9b) provides an improved measure of the strength and duration of El Ninos, La Ninas, and the response to volcanic eruptions. In contrast, use of the calendar year, as in Figure 9a, can be misleading, because one El Nino may coincide well with a calendar year while another is split between two calendar years. The 12-month running mean also provides a better measure of the longevity of an event (a positive or negative temperature excursion).

A clearer view of temporal variations is provided by Figure 10, which covers the shorter period 1950-2010. The top curve is the monthly mean global temperature anomaly and the second curve is the 12-month running mean. The red-blue Nino index is the 12-month running mean of the temperature anomaly (relative to 1951-1980) averaged over the Nino 3.4 area in the Eastern Pacific Ocean [*Philander*, 2006]. Because the monthly Nino index is much smoother than monthly global temperature, we can usefully extend the index to the present. The final point is the 2-month mean (Dec-Jan) Nino 3.4 anomaly, the penultimate point is the 4-month (Oct-Jan) mean anomaly, and so on.

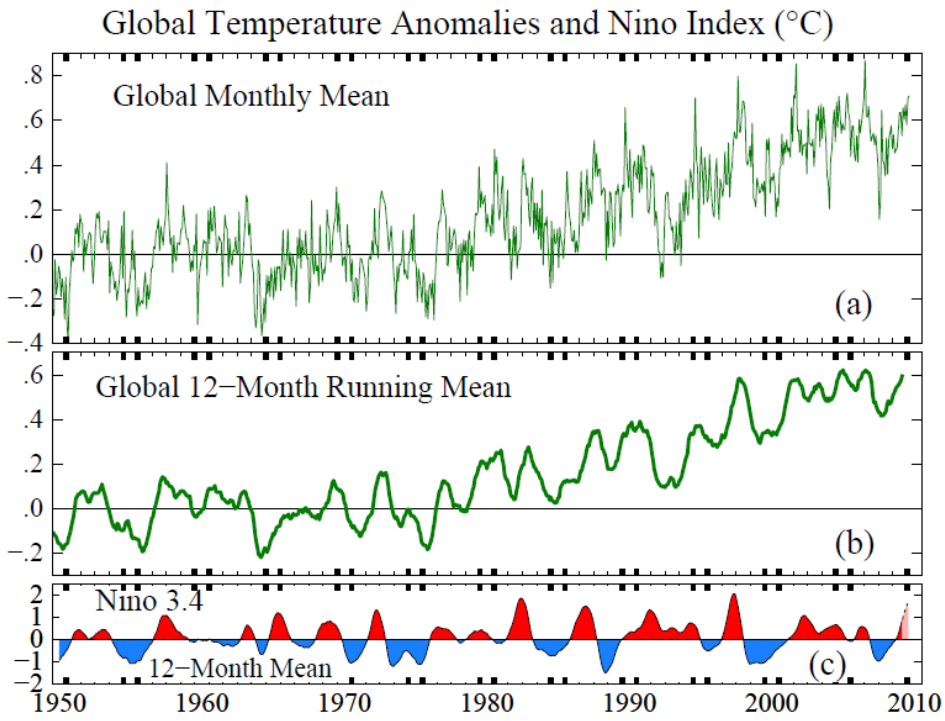

Figure 10. Global monthly and 12-month running mean surface temperature anomalies relative to 1951-1980 base period, and the Nino 3.4 index. Data extend through February 2010.

The well-known strong correlation of global surface temperature with the Nino index is apparent in Figure 10. The correlation is maximum with 12-month running mean global temperature lagging the Nino index by 4 months. Given this lag and the fact that the Nino index has continued to rise in the 6 months since the date of the final 12-month running mean point in Figure 10, it is nearly certain that a new record 12-month global temperature will be set in 2010.

As for the calendar year, it is likely that the 2010 global surface temperature in the GISS analysis also will be a record for the period of instrumental data. However, record global temperature for the calendar year might not occur if El Nino conditions deteriorate rapidly by mid 2010 into La Nina conditions.

7. Comparison of GISS, NCDC and HadCRUT Analyses

Expectation of possible record global temperature raises the question about differences among the several global surface temperature analyses. For example, GISS and NCDC have 2005 as the warmest year in their analyses, while HadCRUT has 1998 as the warmest year. Here we investigate differences arising from two factors that we think are likely to be important: (1) the way that temperature anomalies are extrapolated, or not extrapolated, into regions without observing stations, and (2) the ocean data sets that are employed.

Figure 11 compares the GISS, NCDC, and HadCRUT analyses. The characteristic causing most interest and concern in the media and with the public is their different results for the warmest year in the record, as noted above.

A likely explanation for discrepancy in identification of the warmest year is the fact that the HadCRUT analysis excludes much of the Arctic, where warming has been especially large in

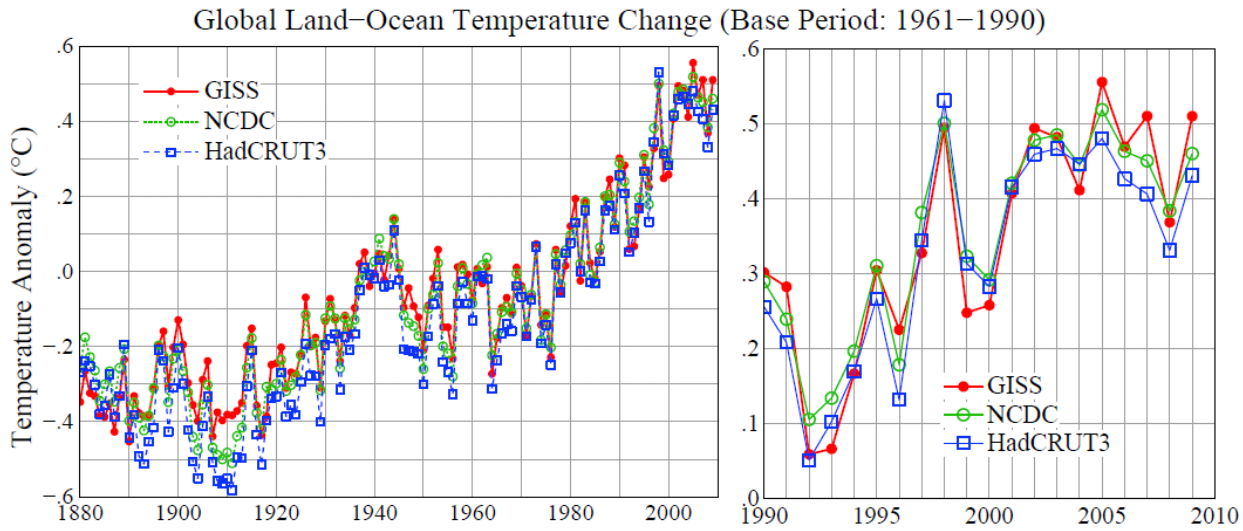

Figure 11. GISS, NCDC and HadCRUT global surface temperature anomalies. Base period is 1961-1990 for consistency with Figures 12 and 13 and base periods used by NCDC and HadCRUT. Last two decades are expanded on the right side.

the past decade, while GISS and NCDC estimate temperature anomalies throughout most of the Arctic. The difference between GISS and HadCRUT results can be investigated quantitatively using available data defining the area that is included in the HadCRUT analysis.

Figure 12 shows maps of GISS and HadCRUT 1998 and 2005 temperature anomalies relative to base period 1961-1990 (the base period used by HadCRUT). The temperature anomalies are at a 5°×5° (latitude-longitude) resolution in Figure 12 for the GISS data to match the resolution of the HadCRUT analysis. In the lower two maps we display the GISS data masked to the same area (and resolution) as the HadCRUT analysis.

Figure 13 shows time series of global temperature for the GISS and HadCRUT analyses, as well as for the GISS analysis masked to the HadCRUT data region. With the analyses limited to the same area, the GISS and HadCRUT results are similar. The GISS analysis finds 1998 as the warmest year, if analysis is limited to the masked area. This figure reveals that the differences that have developed between the GISS and HadCRUT global temperatures during the past decade are due primarily to the extension of the GISS analysis into regions excluded from the HadCRUT analysis.

The question is then: how valid are the extrapolations and interpolations in the GISS analysis? The GISS analysis assigns a temperature anomaly to many gridboxes that do not contain measurement data, specifically all gridboxes located within 1200 km of one or more stations that do have defined temperature anomalies. The rationale for this aspect of the GISS analysis is based on the fact that temperature anomaly patterns tend to be large scale, especially at middle and high latitudes.

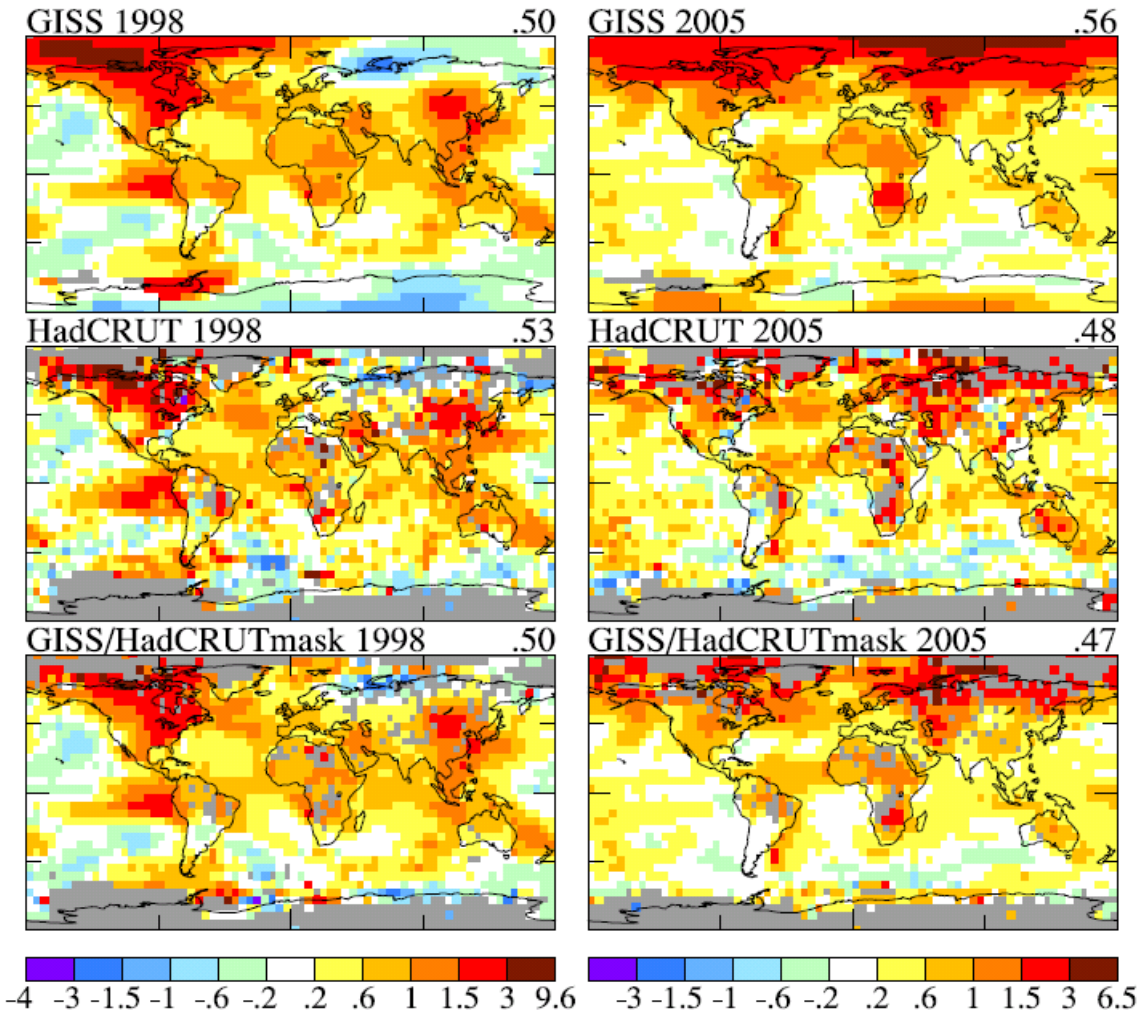

Figure 12. Temperature anomalies (°C) in 1988 (left) and 2005 (right). Top row is GISS analysis, middle row HadCRUT analysis, and bottom row the GISS analysis masked to the same area and spatial resolution as the HadCRUT analysis. Areas without data are gray. "Global" means (upper right corner) are averages over area with data. [Base period is 1961-1990]

The HadCRUT analysis also makes an (implicit) assumption about temperature anomalies in regions remote from meteorological stations, if the HadCRUT result is taken as a global analysis. The HadCRUT approach area-weights temperature anomalies of the regions in each hemisphere that have observations; then the means in each hemisphere are weighted equally to define the global result [*Brohan et al.*, 2006]. Thus HadCRUT implicitly assumes that the Arctic area without observations has a temperature anomaly equal to the hemispheric mean anomaly. Given the pattern of large temperature anomalies in the fringe Arctic areas with data (Figure 12), this implicit estimate would seem to understate Arctic temperature anomalies.

Qualitative support for the greater Arctic anomaly of the GISS analysis is the following. The Arctic temperature anomaly patterns in the GISS analysis, regions warmer and cooler than average when the mean anomaly is adjusted to zero, are realistic-looking meteorological patterns. More quantitative support is provided by satellite observations of infrared radiation

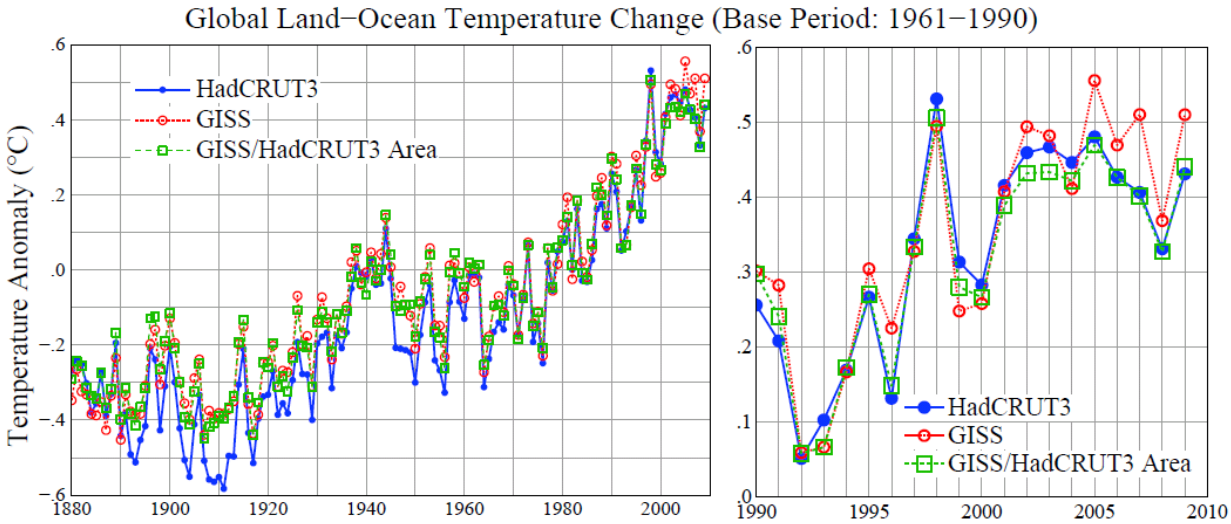

Figure 13. Global surface temperature anomalies (°C) relative to 1961-1990 base period for three cases: HadCRUT, GISS, and GISS anomalies limited to the HadCRUT area.

from the Arctic [*Comiso*, 2006]. Although we have not yet attempted to integrate this infrared data record, which begins in 1981, into our temperature record, the temperature anomaly maps of *Comiso* [2006] have the largest positive temperature anomalies (several degrees Celsius) during the first decade of this century over the interior of Greenland and over the Arctic Ocean in regions where sea ice cover has decreased. Because no weather stations exist in central Greenland and within the sea ice region, our analysis may understate warming in these regions. An exception is the station on Sakhalin Island, which is located in a region of decreasing sea ice cover and which does show relatively large warming in the past decade.

We obtain a quantitative estimate of uncertainty (likely error) in the GISS analysis due to incomplete spatial coverage of stations using a time series of global surface temperature generated by a long run of the GISS climate model runs [*Hansen et al.*, 2007]. We sample this data set at meteorological station locations that existed at several times during the past century. We then find the average error when the model's data for each of these station distributions is used as input to the GISS surface temperature analysis program.

Table 1 shows the derived error. As expected, the error is larger at early dates when station coverage was poorer. Also the error is much larger when data are available only from meteorological stations, without ship or satellite measurements for ocean areas. In recent decades the 2-σ uncertainty (95 percent confidence of being within that range, thus ~2-3 percent chance of being outside that range in a specific direction) has been about 0.05°C. Incomplete coverage of stations is the primary cause of uncertainty in comparing nearby years, for which the effect of more systematic errors such as urban warming is small.

Additional sources of error, including urban effects, become important when comparing temperature anomalies separated by longer periods [*Brohan et al.*, 2006; *Folland et al.*, 2001; *Smith and Reynolds*, 2002]. *Hansen et al.* [2006] have estimated the additional error, by factors other than incomplete spatial coverage, as being $\sigma \approx 0.1$°C on time scales of several decades to a century, but this estimate is necessarily partly subjective. If that estimate is realistic, the total uncertainty in global mean temperature anomaly with land and ocean data included is similar to the error estimate in the first line of Table 1, i.e., the error due to limited spatial coverage when only meteorological stations are available. However, biases due to changing practices in ocean

Table 1. Two-sigma (2σ) error estimate versus time for meteorological stations and land-ocean index

	1880-1900	1900-1950	1960-2008
Meteorological Stations	0.2	0.15	0.08
Land-Ocean Index	0.08	0.05	0.05

measurements may cause even greater uncertainty on the century time scale [*Rayner et al.*, 2006].

In comparisons of nearby years to each other the errors due to changes of measurement practices and urban warming should be small, so the total error in such year-by-year comparisons is probably dominated by the substantial error from incomplete spatial coverage of measurements. Under that assumption, let's consider whether we can specify a rank among the recent global annual temperatures, i.e., which year is warmest, second warmest, etc. Figure 9a shows 2009 as the second warmest year, but it is so close to 1998, 2002, 2003, 2006, and 2007 that we must declare these years as being in a virtual tie as the second warmest year. The maximum difference among these years in the GISS analysis is ≈0.03°C (2009 being the warmest among those years and 2006 the coolest). This total range is approximately equal to our 1σ uncertainty of ≈0.025°C.

The year 2005 is 0.06°C warmer than 1998 in the current GISS analysis including nightlight adjustments. How certain is it that 2005 was warmer than 1998? Given σ ≈ 0.025°C for nearby years, we estimate the probability that 1998 was warmer than 2005 as follows. The actual 1998 and 2005 temperatures are specified by normal probability distributions about our calculated values. For each value of the actual 1998 temperature there is a portion of the probability function for the 2005 temperature that has 2005 cooler than 1998. Integrating successively over the two distributions we find that the chance that 1998 was warmer than 2005 is 0.05, i.e., there is 95 percent confidence that 2005 was warmer than 1998.

The NCDC analysis finds 2005 to be the warmest year, but by a smaller amount. Thus a similar probability calculation for their results would estimate a greater chance that 1998 was actually warmer than 2005. NCDC reports 2009 as being the fifth warmest year (http://www.ncdc.noaa.gov/sotc/?report=global). Although the latter result seems to disagree with the GISS conclusion that 2009 tied for the second warmest year, this is mainly a consequence of the GISS preference to describe as statistical ties those years with global temperature differing by only about one standard deviation or less.

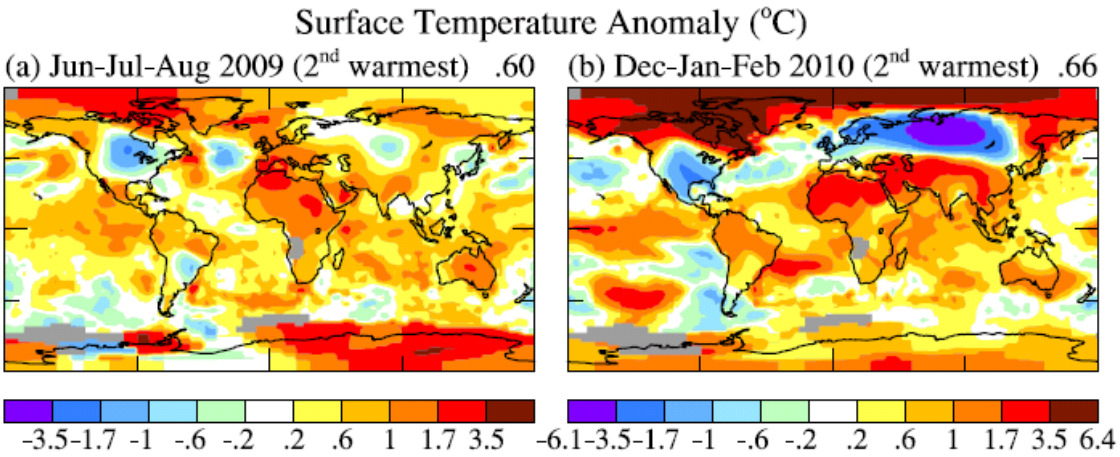

Figure 14. Jun-Jul-Aug 2009 and Dec-Jan-Feb 2010 surface temperature anomalies (°C).

8. Weather variability versus climate trends

Public opinion about climate change is affected by recent and ongoing weather. North America had a cool summer in 2009, perhaps the largest negative temperature anomaly on the planet (Figure 14a). Northern Hemisphere winter (Dec-Jan-Feb) of 2009-2010 was unusually cool in the United States and northern Eurasia (Figure 14b). The cool weather contributed to increased public skepticism about the concept of "global warming", especially in the United States. These regional extremes occurred despite the fact that Jun-Jul-Aug 2009 was second warmest (behind Jun-Jul-Aug 1998) and Dec-Jan-Feb 2009-2010 was second warmest (behind Dec-Jan-Feb 2006-2007).

Northern Hemisphere winter of 2009-2010 was characterized by an unusual exchange of polar and mid-latitude air. Arctic air rushed into both North America and Eurasia, and, of course, was replaced in the polar region by air from middle latitudes. Penetration of Arctic air into middle latitudes is related to the Arctic Oscillation (AO) index [*Thompson and Wallace*, 2000], which is defined by surface atmospheric pressure. When the AO index (Figure 15a) is positive surface pressure is low in the polar region. This helps the middle latitude jet stream blow strongly and consistently from west to east, thus keeping cold Arctic air locked in the polar region. A negative AO index indicates relatively high pressure in the polar region, which favors weaker zonal winds, and greater movement of frigid polar air into middle latitudes.

December 2009 had the most extreme negative Arctic Oscillation since the 1970s. There were ten cases between the early 1960s and mid 1980s with negative AO index more extreme than -2.5, but no such extreme cases since then until December 2009. It is no wonder that the public had become accustomed to a reduction in the extremity of winter cold air blasts. Then, on the heels of the December 2009 anomaly, February 2010 had an even more extreme AO, the most negative AO index in the 1950-2010 period of record (Figure 15).

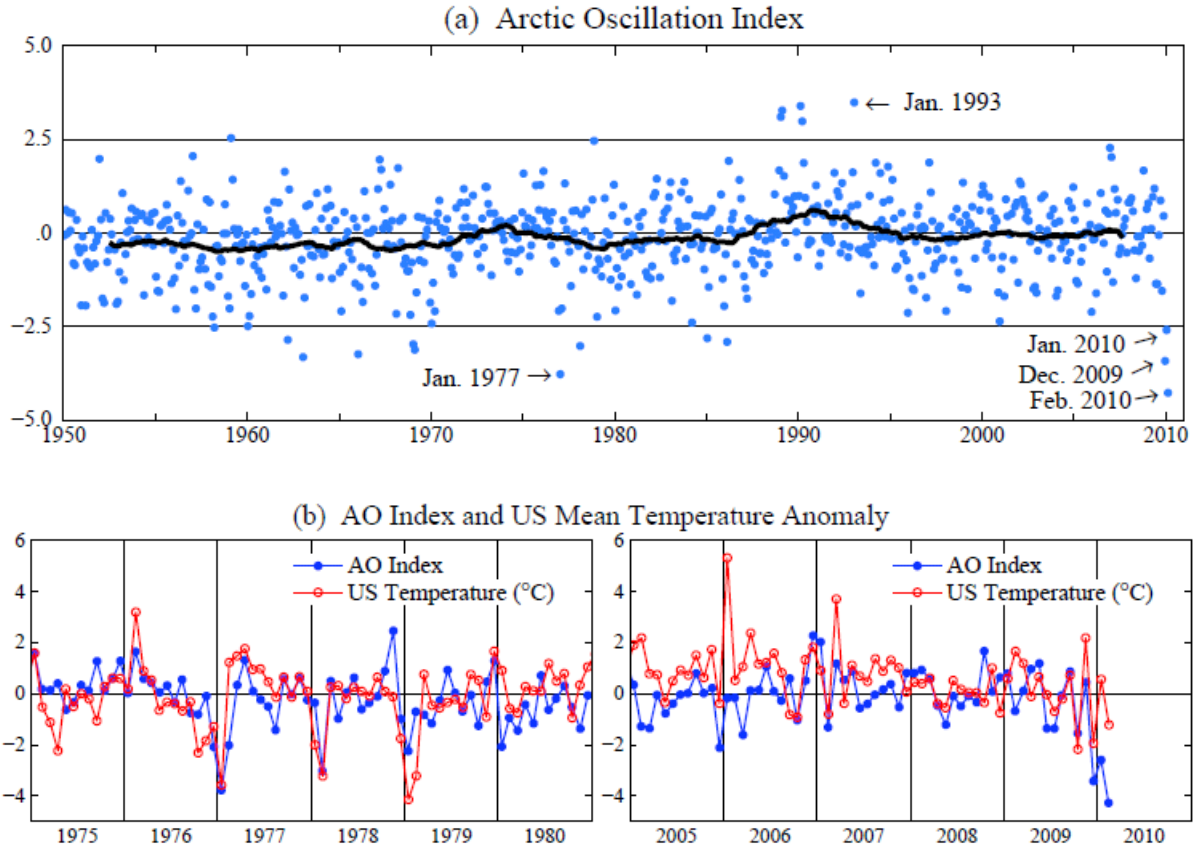

Figure 15. (a) Arctic oscillation (AO) index, data from (**http://www.cpc.noaa.gov/products/precip/CWlink/daily_ao_index/monthly.ao.index.b50.current.ascii.table**). Blue dots are monthly means and black curve is the 60-month (5-year) running mean. (b) AO index at higher temporal resolution and corresponding temperature anomaly in contiguous 48 United States.

The AO index and United States surface temperature anomalies are shown with monthly resolution in Figure 15b for two 6-year periods: the most recent years (2005-2010) and the period (1975-1980) just prior to the rapid global warming of the past three decades. Extreme negative temperature anomalies, when they occur, are usually in a winter month. Note that winter cold anomalies in the late 1970s were more extreme than the recent winter cold anomalies.

Maps of monthly temperature anomalies are shown in Figure 16. Figure 16a is a polar projection for 24-90°N with 1200 km smoothing to provide full coverage, while 250 km resolution without further smoothing is possible for the contiguous United States (Figure 16b) because of high station density there. Note that monthly mean negative anomalies exceeded five degrees Celsius over large areas in the cold months of the late 1970s, while negative temperature excursions are more limited in 2009-2010.

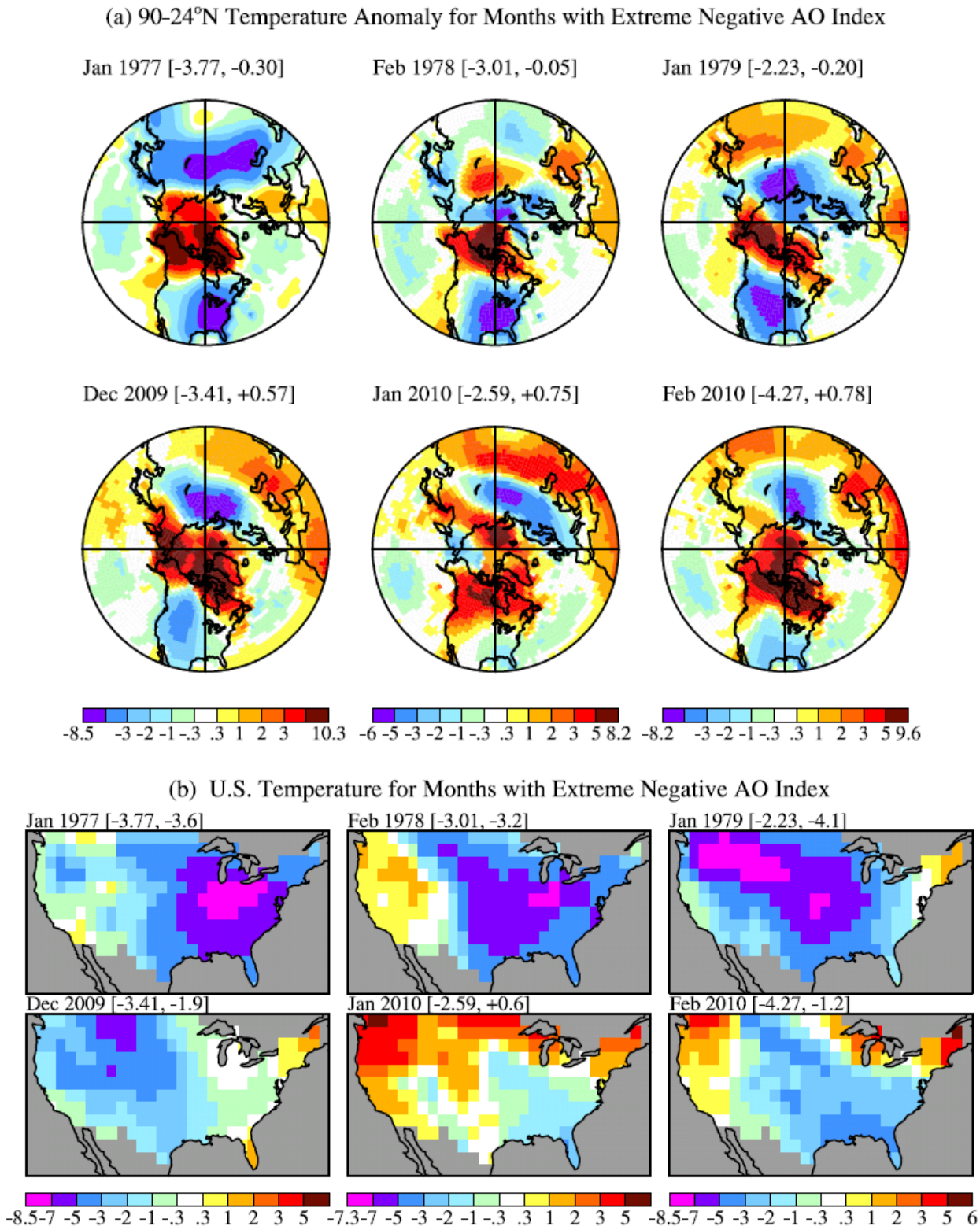

Figure 16. Temperature anomaly from GISS analysis for months with extreme negative AO index. Parenthetical numbers are the AO index and (a) the mean temperature anomaly for 24-90°N and (b) for the contiguous 48 states.

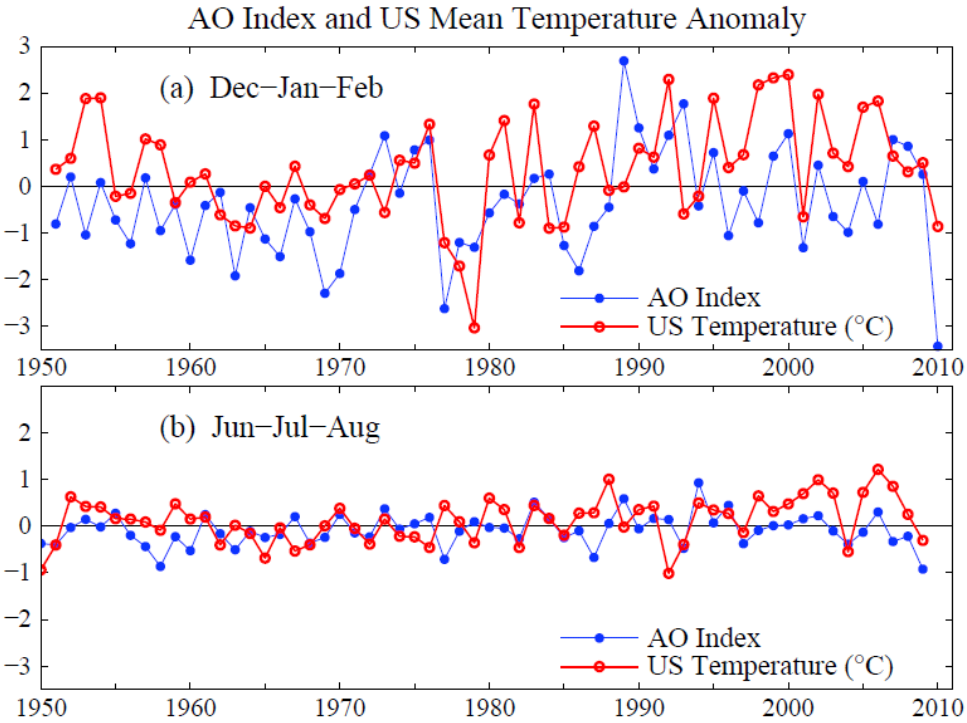

Figure 17. Arctic Oscillation index and United States (48 states) surface temperature anomaly for December-January-February (above) and June-July-August (below).

Monthly temperature anomalies in the United States in the winter are positively correlated with the AO index (Figures 16a and 17a), with any lag between the index and temperature less than the monthly temporal resolution (Figure 16a). *Thompson and Wallace* [2000], *Shindell et al.* [2001] and others point out that increasing carbon dioxide causes the stratosphere to cool, in turn causing on average a stronger polar jet stream and thus a tendency for a more positive Arctic Oscillation.

There is an AO tendency of the expected sense (Figure 16a), but the change is too weak to account for the trend of temperatures. Indeed, Figure 17 shows that the warming trend of the past few decades has led to mostly positive seasonal temperature anomalies, even when the AO is negative. In the United States only one of the past 10 winters and two of the past 10 summers were cooler than the 1951-1980 climatology, a frequency consistent with the expected "loading of the climate dice" [*Hansen*, 1997] due to global warming. Notable change of these probabilities is a result of the fact that local seasonal-mean temperature change due to long-term trends (Figure 18) is now comparable to the magnitude of local interannual variability of seasonal mean temperature (Figure 14b).

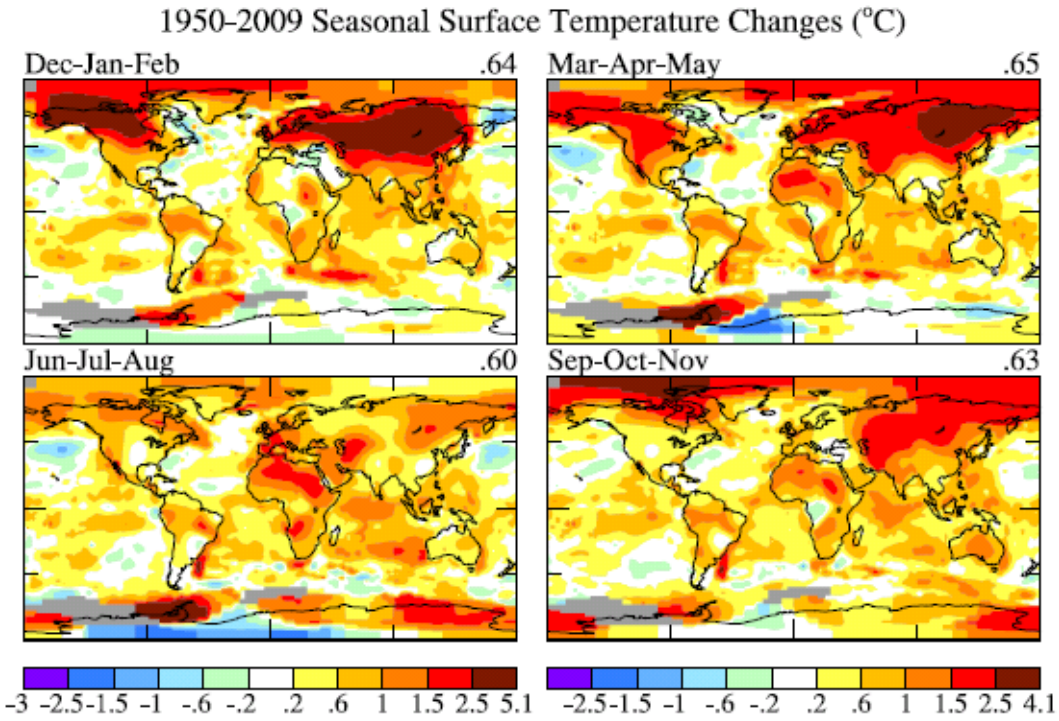

Figure 18. Global maps 4 season temperature anomaly trends (°C) for period 1950-2009.

Monthly temperature anomalies are typically 1.5 to 2 times greater than seasonal anomalies. So loading of the climate dice is not as easy to notice in monthly mean temperature. Daily weather fluctuations are even much larger than global mean warming. Yet it is already possible for an astute observer to detect the effect of global warming in daily data by comparing the frequency of days with record warm temperature to days with record cold temperature. The number of days with record high temperature now exceed the number of days with record cold by about a two to one ratio [*Meehl et al.*, 2009].

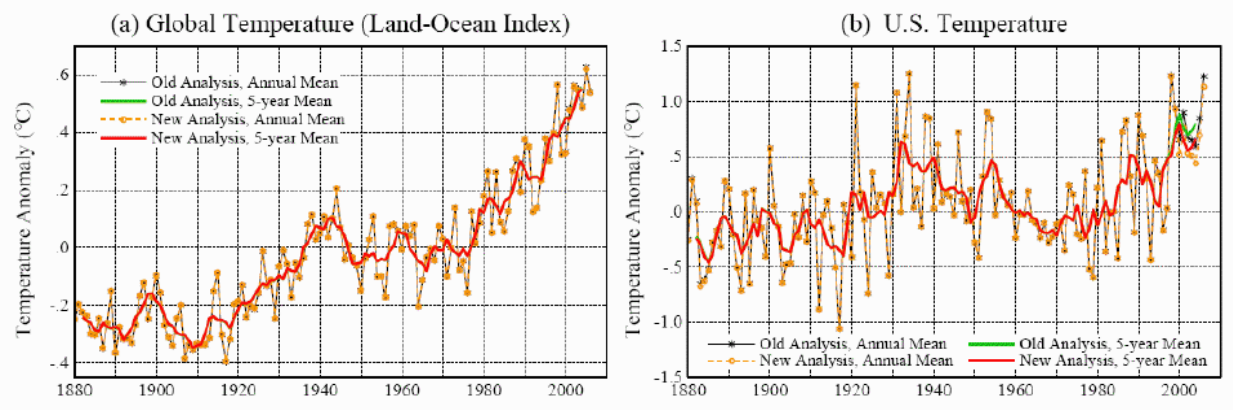

Figure 19. (a) Global and (b) United States analyzed temperature change in the GISS analysis before and after correction of a data flaw in 2007. Results are indistinguishable except post-2000 in the United States.

9. Data flaws

Figure 19 shows the effect of an error that came into the GISS analysis with the changes in the analysis described by *Hansen et al.* [2001]. One of the changes was use of an improved version of the USHCN station data records including adjustments developed by NCDC to correct for station moves and other discontinuities [*Easterling et al.*, 1996]. Our error was failure to recognize that the updates to the records for these stations obtained from NCDC electronically each month did not contain these adjustments. Thus there was a discontinuity in 2000 in those station records, as prior years contained the adjustment while later years did not.

The error was readily corrected, once it was recognized in 2007. Figure 19 shows the global and United States temperatures with and without the error. The error averaged 0.15°C over the contiguous 48 states. Because the 48 states cover only about 1½ percent of the globe, the error in global temperature was about 0.003°C, which is insignificant and undetectable in Figure 19.

This error was widely reported in the media, frequently with the assertion that NASA had intentionally exaggerated the magnitude of global warming, with a further assertion that correction of the error made 1934 the warmest year in the record rather than 1998. Confusion between global and United States temperature was perhaps inadvertent. But as Figure 19 shows the United States temperatures in 1934 and 1998 (and 2006) were and continue to be too similar to conclude that one year was warmer than the other.

Uncertainty in comparing United States temperatures for years separated more than half a century is surely larger than 0.1°C. As shown above, the GISS adjustment for urban effects in the United States by itself approaches that magnitude, even when it is based on USHCN records that are already adjusted by NCDC to account for several sources of bias (inhomogeneity). Their pairwise comparison of urban and rural stations is expected to remove much of the urban effect [*Menne et al.*, 2009].

Temperature records in the United States are especially prone to uncertainty, not only because of high energy use in the United States but also other unique problems such as the bias due to systematic change in the time at which observers read 24-hour max-min thermometers. These problems and adjustments to minimize their effect have been described in numerous papers by NCDC researchers [*Karl et al.* 1986, 1987, 1988, 1989; *Quayle et al.*, 1991; *Easterling et al.*, 1996; *Peterson et al.*, 1997, 1998a, 1998b].

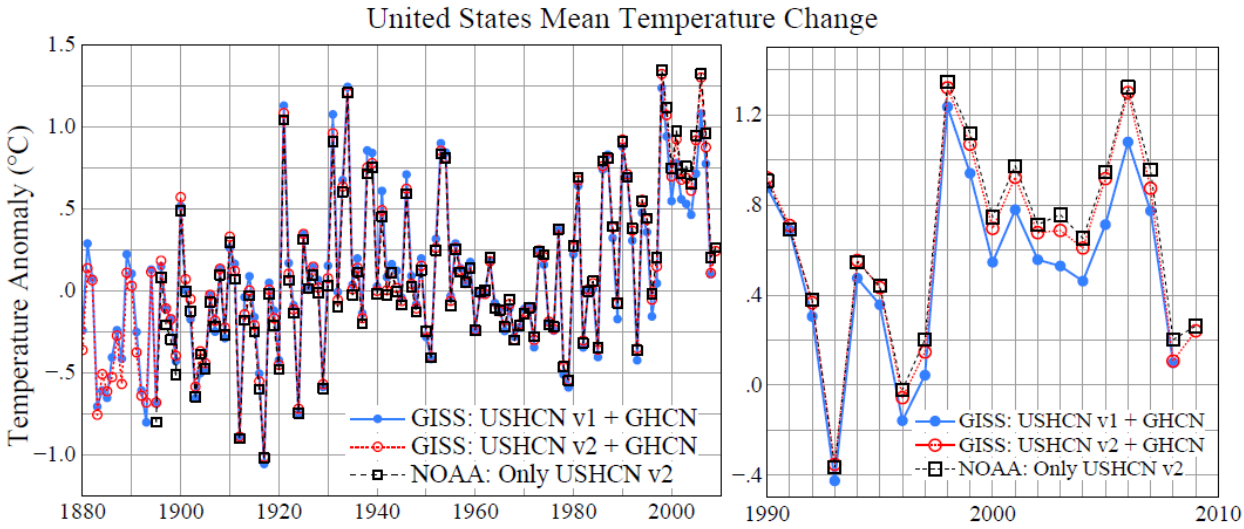

Figure 20. GISS analysis of Untied States temperature change (48 states) using USHCN.v1 (version 1) and USHCN.v2 (v2 became available from NCDC in July 2009; v2 replaced v1 in the GISS analysis in November 2009) and NCDC analysis (web or other reference) for USHCN.v2. NCDC analysis uses only USHCN stations, while the GISS analysis includes use of non-USHCN GHCN stations, with nightlight adjustments of all urban and periurban stations.

When alterations, improvements, or adjustments occur in any of the three input data streams (from meteorological stations, ocean measurements, or Antarctic research stations), the results of the GISS global temperature analysis change accordingly. Monthly updates of the GHCN (including USHCN) data records include not only an additional month of data but late station reports for previous months and sometimes corrections of earlier data. Thus slight changes in the GISS analysis can occur every month, but these are small in comparison with the global and United States temperature changes of the past century or the past three decades.

Occasionally changes of input data occur that are detectable in graphs of the data. This has occurred especially for United States meteorological station data, as NCDC has worked to improve the quality and homogeneity of those records. Figure 20 illustrates the effect of changes in the USHCN data that occurred when we switched (in November 2009) from USHCN version 1 to USHCN version 2, the latter being a NCDC update of their homogenization of USHCN stations). The effect of this revision of USHCN data is noticeable in the United States temperature (Figure 20), but it is small compared to century time scale changes. The effect on global temperature is imperceptible, of the order of a thousandth of a degree.

Based on our experience with the data flaw illustrated in Figure 19, we made two changes to our procedure. First, we now (since April 2008) save every month the complete input data records that we receive from the three data sources. Although the three input data streams are publicly available from their sources, and a record is presumably maintained by the providing organizations, they are now also available from GISS. Second, we published the computer program used for our temperature analysis, which is available on our web site.

An additional data flaw occurred in November 2008. Although the flaw was only present in our data set for a few days (November 10-13), it resulted in additional lessons learned. The GHCN records for many Russian stations for November 2008 were inadvertently a repeat of October 2008 data. The GHCN records are not our data, but we properly had to accept the blame for the error, because the data was used in our analysis. Occasional flaws in input data are normal, and the flaws are eventually noticed and corrected if they are substantial. We have an

effective working relationship with NCDC – reporting to them questionable data that we or our data users discover.

This specific data flaw was a case in point. The quality control program that NCDC runs on the data from global meteorological stations includes a check for repetition of data: if two consecutive months have identical data the data is compared with that at the nearest stations. If it appears that the repetition is likely to be an error, the data is eliminated until the original data source has verified the data. The problem in the November 2008 data evaded this quality check because a change in their program had temporarily, inadvertently, bypassed that quality check.

This data flaw led to another round of fraud accusations on talk shows and other media. Another lesson learned. Since then, to minimize misinformation, we first put our monthly analyzed data up on a site that is not visible to the public. This allows several scientists to examine graphs of the data for potential flaws. If anything seems questionable, we report it back to the data providers for their resolution. This process can delay availability of our data analysis to users for up to several days, and has resulted in a criticism that we "hide" our data.

It is impossible to entirely eliminate data flaws or satisfy all conflicting user demands. We believe that the steps we take now to check the data are a good compromise between assurance of data integrity and prompt availability, and also reasonable from the standpoint of the use of our time and resources. But we welcome user suggestions and any information on possible problems with the data.

Discussion

Human-made climate change has become an issue of surpassing importance to humanity. The most recent report of the United Nations Intergovernmental Panel on Climate Change [*IPCC*, 2007] details the evidence for climate change already underway and the expectation of continued change if fossil fuel use continues to grow.

Global temperature change is the first order manifestation of human-driven climate change, and thus it is understandable that analyses of ongoing global temperature change are now subject to increasing scrutiny and criticisms that are different than would occur for a purely scientific problem. One lesson we have learned is that our approach of making our global data analysis immediately and routinely available, with data use by ourselves and scientific colleagues helping to reveal potential flaws of the input data, has a practical disadvantage: it allows any data flaws to be interpreted as machinations.

The data are too useful for scientific studies not to be made available promptly, however, so we will continue to do that on a monthly basis. Thus we have made the process as transparent as possible, including availability of the computer program that does the analysis, the data that goes into the analysis, and detailed definition of urban adjustment of meteorological station data.

Communicating the reality of climate change to the public is hampered by the large natural variability of weather and climate. Thus, for the sake of early recognition of ongoing climate change, it is important to strive for ways to bring out the climate signal as clearly as possible.

Figure 8 in this paper, decadal mean temperature anomalies, draws attention to the monotonic and substantial changes that are now occurring on the time scale of decades. But because we cannot wait decades for the public to understand the urgency of the matter, we must also seek ways to make the data clearer on shorter time scales.

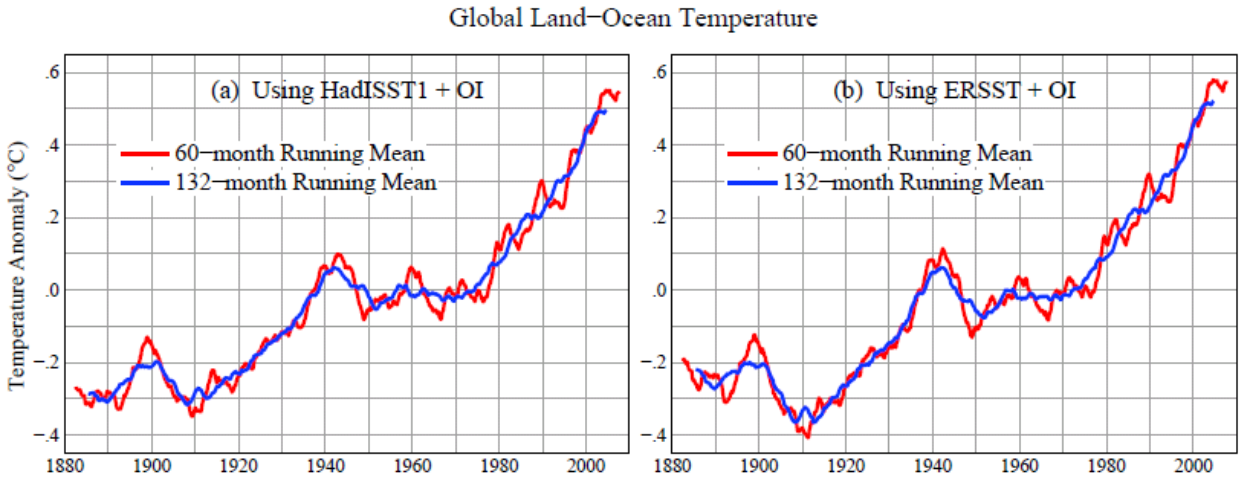

Figure 21. 60-month and 132-month running means through February 2010 for two alternative choices for the ocean data set.

Figures 9b and 10b, the 12-month running mean of global temperature, offer a more powerful way of assessing global climate change than the usual calendar-year mean temperature. The effects of the tropical oscillations between El Ninos and La Ninas can be discerned better in the running mean graph, as well as the effect of large volcanic eruptions such as Mount Pinatubo in 1991. Furthermore, with use of the running mean it is not necessary to wait until January to see the current annual-mean global-mean surface temperature status, because the seasonal cycle is removed by the 12-month running mean just as well at any time of year.

We conclude from these data that a new record global temperature, for the period with instrumental measurements, should be set within the next few months as the effects of the recent and current moderate El Nino continue. This new record temperature will be particularly meaningful because it occurs when the recent minimum of solar irradiance (**http://www.pmodwrc.ch/pmod.php?topic=tsi/composite/SolarConstant**) is having its maximum cooling effect.

The reality of continued global warming contrasts sharply with a frequently heard assertion that the world has been in a cooling trend for the past decade or at least "global warming stopped in 1998." Of course it is possible to find almost any trend for a limited period via judicious choice of start and end dates, but that is not a meaningful exercise. In a wiser assessment, *Solomon et al.* [2009] write "the trend in global surface temperature has been nearly flat since the late 1990s despite continuing increases in the forcing due to the sum of the well-mixed greenhouse gases." But is even that assertion correct?

Climate trends can be seen clearly if we take the 60-month (5-year) and 132-month (11-year) running means, as shown in Figure 21 for data through January 2010. The 5-year mean is sufficient to minimize El Nino variability, while the 11-year mean also minimizes the effect of solar variability. We conclude that there has been no reduction in the global warming trend of 0.15-0.20°C/decade that began in the late 1970s.

References

Brohan, P., J.J. Kennedy, I. Harris, S.F.P. Tett, and P.D. Jones, Uncertainty estimates in regional and global observed temperature changes: A new data set from 1850. *J. Geophys. Res.*, **111**, D12106, doi:10.1029/2005JD006548, 2006.

Christy, J.R., W.B. Norris, and R.T. McNider, Surface temperature variations in East Africa and possible causes. *J. Clim.*, **22**, 3342-3356, 2009.

Comiso, J.C., Arctic warming signals from satellite observations, *Weather*, **61**,70-76, 2006.

Easterling, D.R.,T.C. Peterson, and T.R. Karl, On the development and useof homogenized climate data sets, *J. Clim.*, **9**, 1429-1434, 1996.

Folland, C.K., N.A. Rayner, S.J. Brown, T.M. Smith, S.S.P. Shen, D.E. Parker, I. Macadam, P.D. Jones, R.N. Jones, N. Nichols, and D.M.H. Sexton, Global temperature change and its uncertainties, *Geophys. Res. Lett.*, **28**, 2621-2624, 2001GL012877, 2001

Frölich, C., Solar irradiance variability since 1978. *Space Science Rev.*, **248**, 672-673., 2006

Hansen, J., D. Johnson, A. Lacis, S. Lebedeff, P. Lee, D. Rind, and G. Russell: Climate impact of increasing atmospheric carbon dioxide. *Science*, **213**, 957-966, 1981.

Hansen, J.E., and S. Lebedeff, Global trends of measured surface air temperature. *J. Geophys. Res.*, **92**, 13345-13372, 1987.

Hansen, J., Public understanding of global climate change, pp. 247-253 in *Carl Sagan's Universe*, eds. Y. Terzian and E. Bilson, Cambridge University Press, 282 pp., 1997.

Hansen, J., R. Ruedy, J. Glascoe, and Mki. Sato, GISS analysis of surface temperature change. *J. Geophys. Res.*, **104**, 30997-31022, 1999.

Hansen, J.E., R. Ruedy, M. Sato, M. Imhoff, W. Lawrence, D. Easterling, T. Peterson, and T. Karl, A closer look at United States and global surface temperature change. *J. Geophys. Res.*, **106**, 23947-23963, 2001.

Hansen, J., Mki. Sato, R. Ruedy, K. Lo, D.W. Lea, and M. Medina-Elizade, Global temperature change. *Proc. Natl. Acad. Sci.*, **103**, 14288-14293, 2006.

Hansen, J., M. Sato, R. Ruedy, P. Kharecha, A. Lacis, R.L. Miller, L. Nazarenko, K. Lo, G.A. Schmidt, G. Russell, et al., Climate simulations for 1880-2003 with GISS modelE. *Clim. Dynam.*, **29**, 661-696, 2007 doi:10.1007/s00382-007-0255-8.

Hansen, J., *Storms of My Grandchildren*, Bloomsbury USA, New York, 304 pp., 2009.

Hughes, S.L., N.P. Holliday, E. Colbourne, V. Ozhigin, H. Valdimarsson, S. Osterhus, and K. Wilshire, Comparison of *in situ* time-series of temperature with gridded sea surface temperature datasets in the North Atlantic, ICES j. *Mar. Sci. Adv. Access*, 15 March 2009 doi:10.1093/icesjms/fsp041

Imhoff, M.L., Lawrence, W.T., Stutzer, D.C. and Elvidge, C.D., A technique for using composite DMSP-OLS "city lights" satellite data to map urban area. *Remote Sens. Envir.*, **61**, 361-370, 1997.

IPCC, *Climate Change 2007: The Physical Science Basis*, eds. S. Solomon et al., Cambridge University Press, 996 pp., 2007.

Jones, P.D., S.C.B. Raper, B.S.G. Cherry, C.M. Goodess, and T.M.L. Wigley, Assessment of urbanization effects in time series of surface air temperature over land, *Nature*, **347**, 169-172, 1990.

Karl, T.R., C.N. Williams, P.J. Young, and W.M. Wendland, Model to estimate the time of observation bias associated with monthly mean maximum, minimum and mean temperatures for the United States, *J. Clim Appl. Meteorol.*, **25**, 145-160, 1986.

Karl, T.R., and C.N. Williams, An approach to adjusting climatological time series for discontinuous inhomogeneities, *J. Clim. Appl. Meteorol*., **26**, 1744-1763, 1987.

Karl, T.R., H.F. Diaz, and G. Kukla, Urbanization:Its detection and effect in the United States climate record*, J. Clim*., **1**, 1099-1123, 1988.

Karl, T.R., J.D. Tarplay, R.G. Quayle, H.F. Diaz, D.A. Robinson, and R.S. Bradley, The recent climate record: What it can and cannot tell us, Rev. Geophys., 27, 405-430, 1989.

Karl, T.R., C.N. Williams, and F.T. Quinlan, United States Historical Climatology Network (HCN) Serial Temperature and Precipitation Data. ORNL/CDIAC-30, NDP-019/R1. Carbon Dioxide Information Analysis Center, Oak Ridge National Laboratory, U.S. Department of Energy, Oak Ridge, Tennessee, 1990.

Meehl, G.A., C. Tebaldi, G. Walton, D. Easterling, and L. McDaniel, Relative increase of record high maximum temperatures compared to record low minimum temperatures in the U.S., *Geophys. Res. Lett.*, **36**, L23701, 2009, doi:10.1029/2009GL040736.

Menne, M.J., C.N. Williams, and R.S. Vose, The U.S. historical climatology network monthly temperature data, version 2, *Bull. Amer. Meteorol. Soc.*, **90**, 993-1007, 2009.

National Academy of Sciences (NAS), *Understanding Climate Change*, Washington, DC , 239 pp., 1975.

Parker, D.E., Large-scale warming is not urban, *Nature*, **432**, 290, 2004.

Peterson, T.C. and R. Vose, An overview of the global historical climatology network temperature database, *Bull. Am. Meteorol. Soc.*, **78**, 2837-2850, 1997.

Peterson, T.C., et al., Homogeneity adjustments of in situ atmospheric climate data: A review, *Int. J. Climatol*., **18**, 1493-1517, 1998a.

Peterson, T.C., R. Vose, R. Schmoyer, and V. Razuvaev, Global historical climatology network (GHCN) quality control of monthly temperature data, *Int. J. Climatol.*, **18**, 1169-1179, 1998b.

Peterson, T.C., K.P. Gallo, J. Lawrimore, T.W. Owen, A. Huang, D.A. McKittrick, Global rural temperature trends, *Geophys. Res. Lett.*, **26**, 329-332, 1999.

Peterson, T.C., Assessment of urban versus rural in situ surface temperatures in the contiguous United States: No difference found. *J. Clim*., **16,** 2941-2959, 2003.

Philander, S.G., *Our Affair with El Niño: How We Transformed an Enchanting Peruvian Current into a Global Climate Hazard,* Princeton University Press, Princeton, 288 pp., 2006.

Quayle, R.G., D.R. Easterling, T.R. Karl, and P.Y. Hughes, Effects of recent thermometerchanges in the cooperative station network, *Bull. Amer. Meteorol. Soc*., **72**, 1718-1724, 1991.

Rayner, N.A., D.E. Parker, E.B. Horton, C.K. Folland, L.V. Alexander, D.P. Rowell, E.C. Kent, et al., Global analyses of sea surface temperature, sea ice, and night marine air temperature since the late nineteenth century, *J. Geophys. Res,.* **108**, 4407, 2003 doi: 10.1029/2002JD002670.

Rayner, N.A., P. Brohan, D.E. Parker, C.K. Folland, J.J. Kennedy, M. Vanicek, T.J. Ansell, and S.F.B. Tett, Improved analyses of changes and uncertainties in sea surface temperature measured in situ since the mid-nineteenth century: the HadSST2 dataset, *J. Clim.,* **19**, 446-469, 2006.

Reynolds, R.W., N.A. Rayner, T. M. Smith, D.C. Stokes, and W. Wang, An improved *in situ* and satellite SST analysis for climate, *J. Clim.,* **15**, 1609-1625, 2002.

Shindell, D., G.A. Schmidt, R.L. Miller, and D. Rind, Northern Hemispherre winter climate response to greenhouse gas, volcanic, ozone and solar forcing, *J. Geophys. Res.*, **106**, 7193-7210, 2001.

Smith, T.M., and R.W. Reynolds, Bias corrections for historic sea surface temperatures based on marine air temperatures, *J. Clim.*, **15**, 73-87, 2002.

Smith, T.M., R.W. Reynolds, and J. Lawrimore, Improvements to NOAA's historical merged land-ocean surface temperature analysis (1880-2006), *J. Clim.,* **21**, 2283-2296, 2008.

Solomon, S., K. Rosenlof, R. Portmann, J. Daniel, S. Davis, T. Sanford, and G.K. Plattner. *ScienceExpress*, 10.1126/science.1182488, 28 January 2010.

Thompson, D.W.J., and J.M. Wallace, Annular modes in the extratropical circulation: Part I: Month-to-month variability, *J. Clim.,* **13**, 1000-1016, 2000.

Thompson,D.W.J., J.J. Kennedy, J.M. Wallace, and P.D. Jones, A large discontinuity in the mid-twentieth century in observed global-mean surface temperature, *Nature*, **453**, 646-649, 2008.

Turner, J., S. R. Colwell, G. J. Marshall, T. A. Lachlan-Cope, A. M. Carleton, Phil D. Jones, V. Lagun, P. A. Reid, and S. Iagovkina, The SCAR READER project: Toward a high quality database of mean Antarctic meteorological observations. *J. Clim.*, **17**, 2890-2898, 2004.

Worley, S.J., S.D. Woodruff, R.W. Reynolds, S.J. Lubker, and N. Lott, ICOADS release 2.1. data and products. *Int. J. Climatol.*, **25**, 823-842, 2005.

Supplementary Material

The global temperature change obtained in our analysis depends on the ocean surface temperature data set(s) that we employ. Although these data sets are described by the groups who have produced them, the differences among the data sets have not been compared in detail to our knowledge. Here we compare the HadISST1, ERSST, and HadSST2 data sets, as well as the data sets that result when OI satellite data are concatenated with HadISST1 or ERSST.

Figure S1 compares the HadISST1, HadSST2 and ERSST data sets after spatial averaging. The top row is the temperature anomaly averaged over only those regions where all three records have data. The lower graphs are estimates of the global ocean mean anomaly, obtained as follows: monthly SSTs are interpolated to 5°x5° grid (HadSST2 grid), mean anomalies are computed for the permanently ice-free ocean area with defined SST within each of four latitude zones (90-25°S, 25-0°S, 0-25°N, 25-90°N), the global-ocean mean is computed as the average of these four zones with each weighted by the open-ocean area of that zone.

Variations among the resulting data sets are within the expected uncertainty ranges [*Folland et al.*, 2001; *Rayner et al.*, 2006; *Reynolds et al.*, 2002; *Smith et al.*, 2008]. It is notable that the largest differences occur in the past decade, when the most comprehensive observations exist. Figure S2 shows the geographical distribution of the differences between the data sets.

The largest difference between HadSST2 and HadISST1, as well as the largest difference between ERSST and HadISST1, occurs in the upwelling region just west of South America. Presumably this change from the earlier HadISST1 is a result of the more comprehensive data available from ICOADS release 2.1 [*Worley et al.*, 2005]. However, HadSST2 and ERSST are also warmer than HadISST1 during the past decade throughout most of the global ocean. The ubiquity of the recent differences suggests that they may be related to calibration of satellite measurements, which are a major data source in the past decade.

The effect on the GISS analysis of global temperature change caused by alternative choices for the ocean data record is reduced by the fixed contributions from meteorological stations on continents and islands, including extrapolation into the Arctic. Figure 6 compares the global temperature records that result with HadISST1+OI and ERSST, the differences being as much as several hundredths of a degree Celsius.

The standard GISS global analysis uses the concatenated HadISST1+OISST data set, as described in the main text. Any of the alternative ocean data sets that we have described here would yield slightly greater global warming, both in recent decades and on the century time scale.

Until improved assessments of the alternative SST data sets exist, the GISS global analysis will be made available for both HadISST1 and ERSST, in both cases with these long-term data sets concatenated with OISST for 1982-present. HadISST1+OISST will continue to be our standard product unless and until verifications show ERSST to be superior.

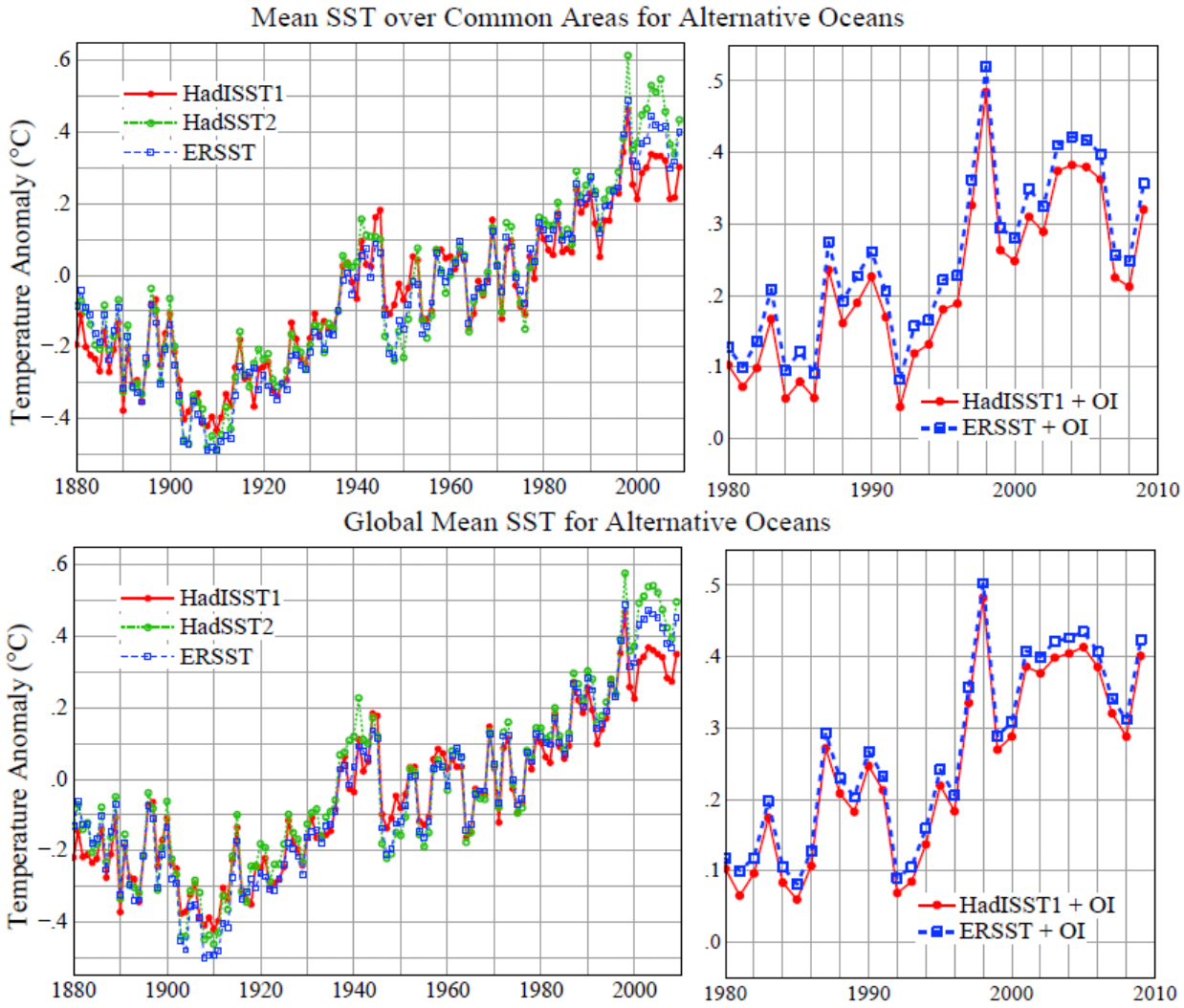

Figure S1. Ocean surface temperatures for alternative data sets, the temperature zero point in all cases being the 1951-1980 (base period) mean. In the graphs on the right OI is concatenated by equating its mean for 1982-1992 with the mean of the appended data set for the same period. The top row uses only areas that have data in all data sets; the temperature anomaly is averaged over this area, so it is not a true global ocean mean. The bottom row is the global ocean mean obtained for each of these data sets, as described in the text.

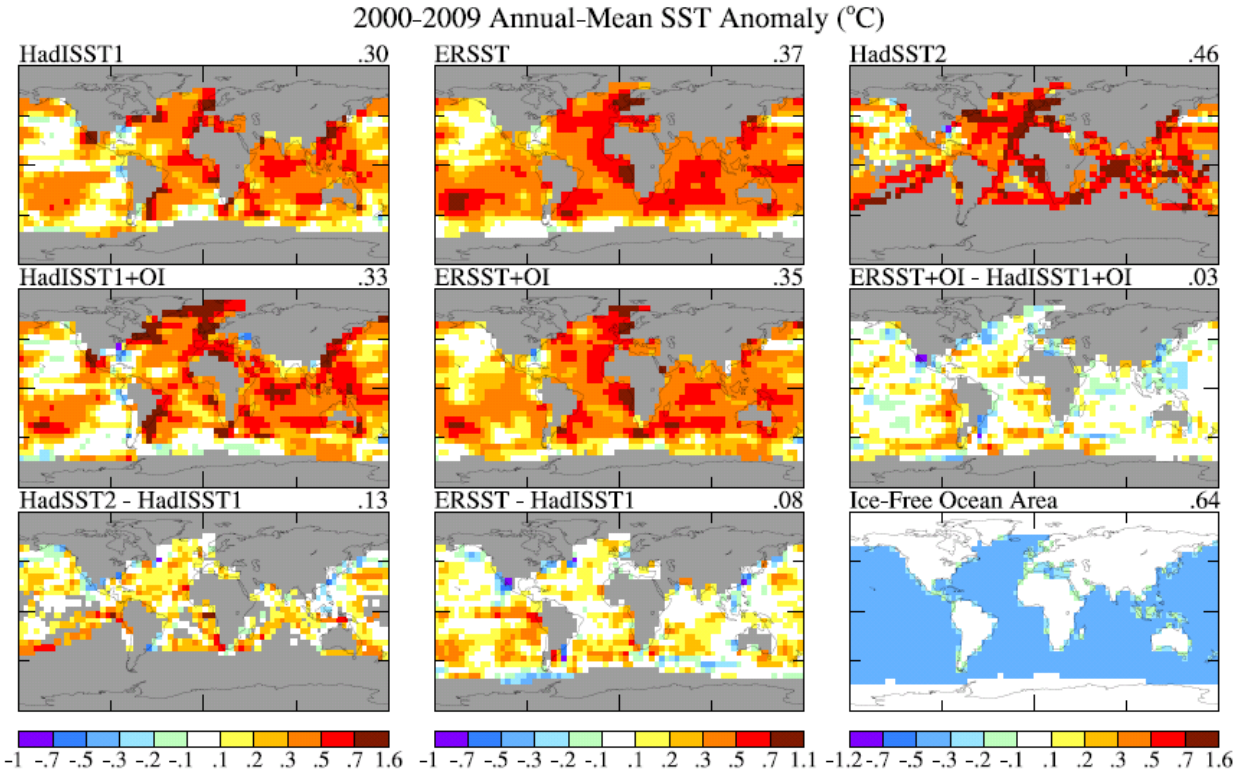

Figure S2. SST 2000-2009 anomalies for several data sets and their differences. The final map shows the permanently ice-free area used in computing the global ocean mean temperature.